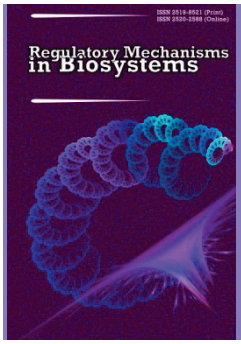

Regulatory Mechanisms in Biosystems

ISSN 2519-8521 (Print)
ISSN 2520-2588 (Online)
Regul. Mech. Biosyst.,
2023, 14(4), 634–651
doi: 10.15421/022392

The structure of beta-diversity explains why the relevance of phytoindication increases under the influence of park reconstruction

K. O. Molozhon*, O. I. Lisovets**, O. M. Kunakh**, O. V. Zhukov*

**Bogdan Khmelnitsky Melitopol State Pedagogical University, Melitopol, Ukraine*
***Oles Honchar Dnipro National University, Dnipro, Ukraine*

Article info

Received 01.08.2023
Received in revised form 02.09.2023
Accepted 12.09.2023

Bogdan Khmelnitsky Melitopol State Pedagogical University, Hetmanska st., 20, Melitopol, 72318, Ukraine.
Tel.: +38-068-154-15-78.
E-mail: nadyayork777@gmail.com

Oles Honchar Dnipro National University, Gagarin av., 72, Dnipro, 49000, Ukraine.
Tel.: +38-098-858-23-79.
E-mail: kunah_olga@ukr.net

Molozhon, K. O., Lisovets, O. I., Kunakh, O. M., & Zhukov, O. V. (2023). The structure of beta-diversity explains why the relevance of phytoindication increases under the influence of park reconstruction. Regulatory Mechanisms in Biosystems, 14(4), 634–651. doi:10.15421/022392

Urbanization causes the highest local extinction rates and often leads to the loss of the vast majority of native species. Plant communities are sensitive to urban expansion and are therefore indicators of human land use. A city park, part of which has undergone reconstruction, was studied. The study found that the changes in ecological conditions caused by the reconstruction of a city park can be detected using phytoindication. The informativeness of phytoindication scales was shown to increase under conditions of anthropogenic load. The phytoindication scales are a reliable source of information for assessing the state of the vegetation cover of park plantations. The ecological regimes were assessed based on descriptions of the vegetation cover using Didukh's phytoindication scales. The phytoindication approach allows one to identify changes in ecological regimes that occur as a result of park reconstruction and to separate them from ecological regimes of natural origin. The study showed that the reconstruction of the park significantly affects the conditions of the park and the diversity of vegetation. The ratio of useful phytoindicative information compared to information noise in the structure of beta-diversity of the park's plantations increases significantly as a result of the park's reconstruction. The reconstruction of the park has led to changes in the spatial organization of the vegetation cover. The results obtained indicate a decrease in soil moisture as a result of the park's reconstruction. The park's reconstruction leads to a significant change in the light regime of the park's plantings, which leads to changes in the park's vegetation and soils. Reducing the density of plantations as a result of their pruning during the reconstruction process also decreases the amount of fallen leaves that form leaf litter. A significant increase in the variability of the moisture regime under the influence of the park reconstruction was found. The phytoindication revealed a decrease in the acidity of the soil solution as a result of the reconstruction. The changes in soil acidity are accompanied by an increase in phytoindication estimates of carbonate content in the soil. The observed increase in carbonate content estimates may be an artifact when representatives of another ecological group also have related ecological properties that can be misinterpreted as indicators of certain regimes. The phytoindication also revealed trends in the variability of microclimatic conditions in the park as a result of reconstruction. The reconstruction of the park leads not only to a change in the modal levels of ecological regimes, but also to the formation of specific patterns of their spatial distribution. The heterogenization of the ecological space under the influence of reconstruction has been established. This heterogenization is evident in the fact that areas with homogeneous vegetation cover are decreasing. The accuracy of the description of the spatial process was found to have decreased after the park reconstruction procedures. Smooth spatial structures of the park's vegetation cover without reconstruction are changing into rough spatial structures of the park after reconstruction. The park's reconstruction obviously disrupts the course of long-term processes that structure the vegetation cover, which leads to temporal and spatial desynchronization of the dynamics of ecological processes. The spatial variation of variables that indicate soil processes can best be described. In contrast, the phytoindication scales that indicate climatic factors are much less spatially structured. The best variogram model to describe the spatial process is also changing under the influence of reconstruction. The significant consequences of the park reconstruction are time variability and spatial heterogeneity of ecological processes.

Keywords: recreation; GIS; innovation project; spatial ecology; ecosystem transformation; plant ecology; biometry; human ecology.

Introduction

Cities are expanding around the world, and urbanization is believed to be a global danger to biodiversity. Urban areas are "hot spots" causing environmental changes at different levels. Among the many human activities that trigger a loss of habitat, urbanization causes some of the highest local extinction rates and often leads to the disappearance of the vast majority of native species (Vale & Vale, 1976). The physical requirements of manufacturing and human consumption are changing land use and vegetation patterns, biodiversity and hydrosystems at local and regional levels, and urban pollution is affecting biogeochemical cycles and climate at local and global levels (Grimm et al., 2008). Urban habitats worldwide are becoming increasingly similar in structure and composition, leading to a homogenisation of ecosystem functions (Pickett et al., 2011; Faly & Brygadyrenko, 2014; Putchkov et al., 2019). Physical and biological parameters of urban environments change consistently along urbanisation gradients (Seto et al., 2010). Increasing urbanisation reduces species diversity, richness and evenness of plant communities (Alue et al., 2022). Urbanization creates a special environment in cities at the meso and local scale (Sharifi, 2019), where the key abiotic conditions and resources affecting the productivity of plants, such as temperature (Li et al., 2019), light intensity (Ding et al., 2022), water and carbon dioxide availability (Ruas et al., 2022), physical and chemical properties of the soil (Enescu et al., 2022) are significantly different from the surrounding non-urban landscape (Williams et al., 2015).

Species interactions are the basis of ecological communities and are important for population and community dynamics, and for the generation, maintenance and structure of biodiversity (Theodorou, 2022). Urbanisation can also alter biotic interactions and disturbance regimes by causing localised extinctions and introducing new organisms (Williams et al., 2015). Each of these changes can potentially act as a biotic ecological filter or stressor, affecting plant species differently depending on their ecological niche and the traits they have evolved to exploit it. Common environmental changes due to urbanisation include climate warming due to the urban heat island effect (Sumasgutner et al., 2023). Parkland is the best way to reduce the negative effects of climate change in cities (Ullah et al., 2023). Buildings, especially in the industrial zone, contribute significantly to the increase in the Earth's surface temperature. The negative correlation between surface temperature and NDVI suggests that green spaces mitigate the warming effect in cities. Built-up or paved areas lead to urban heat islands (Rashid et al., 2022). Soils in urban areas are becoming more alkaline, drier and richer in nutrients and organic matter due to the combined effects of impervious surfaces and aerial deposition of nutrients (Asabere et al., 2018). The increase in total impervious surface area is the main factor influencing soil alkalisation in urban forests(Zhang et al., 2023).

Plant communities respond sensitively to the expansion of cities and therefore provide indicators of human land use. A major issue with urban growth is that it replaces native species that are being lost with widespread "weedy" non-native species. Cities facilitate biological invasions because invasive species are more frequent in cities and because they are more successful in disturbed environments. This substitution is a process of biotic homogenisation that threatens to reduce the biological distinctiveness of regional ecosystems (McKinney, 2006). Studies on urban gradients show that for many taxa, such as plants (Kowarik, 1995), birds and butterflies (Blair & Launer, 1997), the number of non-native species increases towards the centers of urbanisation, while the number of native species decreases. Vegetation diversity depends on the distance to the city center of land use types and the percentage of development. The structure of life forms and different evolutionary strategies of plants is influenced by the characteristics of the urban landscape (Vakhlamova et al., 2014). Species richness of mammals, reptiles, amphibians, invertebrates and plants tends to decrease in areas with extreme urbanisation. The impact of moderate urbanisation varies considerably between groups. Most plant studies indicate an increase in species richness with moderate urbanisation, while only a minority of invertebrate studies and a very small minority of non-avian vertebrate studies show an increase in species richness. Importation of non-native species, spatial heterogeneity, intermediate disturbance and scale are considered to be the main factors affecting species richness within an urban area (McKinney, 2008).

The Ellenberg indicator species system is widely accepted and applied to evaluate the climate, light and soil conditions in Central Europe and beyond (Dyderski et al., 2017). The Ellenberg indicator values are widely used for various environmental analyses due to their numerous confirmed correlations with the instrumental measurements of environmental parameters (Schaffers & Sýkora, 2000). The correlation between the light, soil acidity and nitrogen indicators and the measured light intensity, soil pH and cation exchange capacity increased with forest age. The Ellenberg indicator values were relatively good predictors of ecological conditions in ancient virgin forests with a stabilised species composition, which was determined mainly by the ecological regime. However, they were much weaker indicators in young forests (Dzwonko, 2001). Indicator values are highly reliable and can complement or, in some cases, replace measurements to determine the values of environmental variables and monitor their changes (Diekmann, 2003). In urban conditions, phytoindicator assessments indicate that, compared to large forests, small forest areas have drier, more nutrient-rich and less acidic soil (Godefroid & Koedam, 2003). Species more common in the urban environment have higher phytoindicator optima for soil pH and soil nitrogen content (Vallet et al., 2008). Analysis using the Ellenberg scales has shown that non-native species in forests tend to occur in the areas with relatively high nitrogen availability and soil reaction (Yakovenko et al., 2023). Therefore, an increase in nitrogen availability, including through increased atmospheric deposition, can facilitate the spread of invasive species (Zerbe & Wirth, 2006). The phytoindication indicates the combined effects of eutrophication and anthropogenic transformation, which lead to a decrease in the diversity of the plant cover. Nutrient inputs lead to an increase in the availability of nutrients for plants, which promotes the growth of tall and competitive grasses that outcompete other plant species (Mölder & Schneider, 2010). The dynamics of habitat conditions in forested and non-forested ecosystems under conditions of spontaneous regeneration was established using the Ellenberg scales (Woziwoda & Kopeć, 2014). Phytoindication made it possible to identify the specific environmental conditions under which the invasive species have an advantage for spreading compared to the native ones. Among these factors, the increased nitrogen content and lower soil acidity are the leading ones (Halarewicz & Żołnierz, 2014). Phytoindication scales can be used for small-scale mapping, including anthropogenically transformed areas (Didukh et al., 1997). Phytoindication scales can also be used to interpret ordination axes (Persson, 1981). The statistical conclusions from the analysis of the relationship between the average values of indicator parameters and other variables derived from species composition can lead to highly biased results and misinterpretation (Zelený & Schaffers, 2012). The indicator scores contain the ecological information derived from the indicator values, which is independent of data on the composition of plant communities and comes from expert knowledge of the ecological optima of species. The indicator values can be used as the explanatory variables in constrained ordination (RDA or CCA). The Ellenberg ecological indicators have been criticised for not being distinguishable from a random distribution and for their poor performance in anthropogenically disturbed areas (Dzwonko, 2001).

The aim of the study was to test the following hypotheses: 1) the changes in environmental conditions induced by the reconstruction of an urban park can be identified using phytoindication; 2) the reconstruction of the park is a driver of changes in vegetation cover at the level of individual polygons as well as within individual polygons; 3) the information relevance of phytoindication scales increases under conditions of anthropogenic disturbance.

Materials and methods

Sample fields. The survey was carried out in the recreational zone of the Botanical Garden of the Oles Honchar Dnipro National University (Ukraine) (48.43˚ N 35.05˚ E). More information on the features of the field experiment was provided in our previous article (Zhukov et al., 2023). The city park was reconstructed over an area of 2.8 ha. The vegetation cover was described within two polygons in the reconstructed area (polygons a, b) and within two polygons from the area where the park was not reconstructed (c, d). The procedure for selecting control polygons without reconstruction is described in our previous article (Kunakh et al., 2021). The polygon consisted of 105 sample points. The points were located along 7 transects of 15 points each. The distance between points in a transect, as well as the distance between transects, was 3 m. Thus, the vegetation was described in 105 squares of 3×3 meters in each of the polygons. The projected plant cover was assessed visually. All species were identified to species level in all plots. Seedlings and saplings of tree species were subsequently excluded from the analysis. Plant taxonomy based on Euro+Med Plantbase (http://ww2.bgbm.org/EuroPlusMed).

Phytoindication assessment of ecological regimes. The ecological regimes were assessed on the basis of vegetation cover descriptions using the Didukh (2011) phytoindication scales. The phytoindication scales include edaphic and climatic scales. The edaphic scales of phytoindication include soil water regime (Hd), moisture variability (fH), soil aeration (Ae), soil acidity (Rc), total salt regime (Sl), soil carbonate content (Ca) and soil nitrogen content (Nt). The climate scales include parameters of thermal climate (thermal regime, Tm), humidity (Om), cryoclimate (Cr) and continentality (Kn). Additionally, there is a light scale (Lc), which is recognized as a microclimate scale. The phytoindication assessment of environmental factors was carried out using the Buzuk ideal indicator method (Buzuk, 2017). The plant ecological groups are divided into 23 gradations according to their relation to the humidity regime (Didukh, 2011). The scores of the moisture regime can be translated into phytoindication estimates of the productive moisture stock in the one-meter soil layer using the formula (Maslikova, 2018b):

$$W = 18.65\, exp(0.15H),$$

where W is the content of productive moisture in the one-meter layer of soil (mm); H is a score of the moisture regime. The content of productive moisture in a meter layer of less than 60 mm is considered very low, the content in the range of 60–90 mm is considered low, the content in the range of 90–130 mm is considered satisfactory, the content in the range of 130–160 mm is considered good and the content in the range of more than 160 mm is considered very good (Vadunina & Korchagina, 1986).

The plant ecological groups were divided into 12 gradations according to their relation to the variability of the moisture regime. The scores can be translated into the value of the coefficient of irregularity of moisture ω, which varies from 0 (the lowest level of contrast in moisture conditions of constantly moist or constantly dry habitats) to 0.5 (the highest level of contrast in moisture conditions where conditions of almost complete immersion in water are followed by drought) (Maslikova, 2018):

$$\omega = 0.042fH - 0.032,$$

where ω is the coefficient of irregularity of moisture, fH is a score of the variability of the moisture regime.

The plant ecological groups were divided into 15 gradations according to their relationship to the aeration regime. The scores can be translated into the value of air-filled porosity percentage of the total porosity volume as follows (Maslikova, 2018):

$$P = \frac{100 - Ae^4}{100 * (Ae^4 - 1700)},$$

where P is the air-filled porosity percentage (% of the total volume of the pore space in the soil); Ae is the score of the aeration regime.

The plant ecological groups are divided into 15 gradations according to their relationship to soil acidity. The scores can be converted to the pH of the soil aqueous solution as follows (Maslikova, 2018c):

$$\mathrm{pH} = 2.26 \ln(Rc) + 1.88,$$

where pH is the negative logarithm of the concentration of hydrogen ions in the soil solution, Rc is the acidity score.

The plant ecological groups are divided into 19 gradations according to their relationship to the total salt regime. The scores can be translated into water-soluble salt content as follows (Maslikova, 2018c):

$$S = 2^{0.6Sl+1},$$

where S is the salt content in the soil solution (μg/L); Sl is the score of the soil salinity regime.

The plant ecological groups were divided into 13 gradations according to their relationship to the carbonate content of the soil. The scores can be converted to CaO+MgO content as follows (Maslikova et al., 2019):

$$\mathrm{CaO} + \mathrm{MgO} = 14\frac{Ca^{4.5}}{Ca^{4.5} + 45000},$$

where CaO+MgO is the carbonate content (in terms of calcium and magnesium oxides, %); Ca is a score for carbonate content.

The plant ecological groups are divided into 11 gradations according to their relationship to soil nitrogen content. The scores can be converted to soil nitrogen content as follows (Maslikova et al., 2019):

$$N = 5\frac{Nt^{3.7}}{Nt^{3.7} + 345},$$

where N is the nitrogen content in the soil (g/kg); Nt is a score for the soil trophic regime.

The plant ecological groups are divided into 17 gradations according to their relationship to the thermal regime. The scores can be translated into a radiation balance as follows:

$$RB = 0.21\,Tm,$$

where RB is the radiation balance (gJ/m^2 year); Tm is the thermal regime score. It should be noted that if the radiation balance is presented in Kcal/cm^2 year, then it is enough to multiply the score by 5.

The plant ecological groups are divided into 23 gradations according to their relationship to the atmospheric humidity regime. The ombroclimate scores can be translated into the difference in the amount of precipitation before evaporation from the open water surface per year in terms of average days:

$$Hum = 0.54\,Om - 7,$$

where Hum is the difference between the average annual precipitation per day and evaporation from the open water surface over the same period, mm; Om is the climate humidity score.

The plant ecological groups are divided into 17 gradations according to their relationship to continentality. The continentality scores can be converted to the Ivanov (1959) continentality scale as follows:

$$SKn = 10\,Kn + 41,$$

where *SKn* is the Ivanov continentality scale, *Kn* is the score of the continentality regime.

The plant ecological groups are divided into 15 gradations according to their relationship to the cryoclimate. The cryoclimate scores can be converted to the average temperature of the coldest month of the year as follows:

$$Temp = 3.83\,Cr - 38.17,$$

where *Temp* the average temperature of the coldest month of the year (°C); *Cr* is a score for the cryoclimate.

The lighting regime is assessed in terms of phytoindication scores, and so far the procedure for converting to physical indicators has not been proposed.

Geostatistical analysis. The application of kriging to the construction of spatial models is widely used in geostatistics (Minasny & McBratney, 2005a). The variogram is a key concept in geostatistics. It provides crucial insights into the appropriate mathematical form of the variogram and allows the spatial variation to be accurately assessed (McBratney & Pringle, 1999), which is the precondition to predict the variability of ecological features at the local or regional level (Minasny & McBratney, 2005a). The variogram distinguishes between the spatial component of the attribute's variability and the spatially independent component. The intersection of the model variogram curve with the ordinate axis is called a nugget (τ^2). A nugget indicates the variability of a feature independent of space. The difference between the asymptote and the nugget is called the sill (σ^2). The sill indicates the spatially dependent component of the feature's variability. The influence of spatial interactions decays with distance, which is represented by the range. The distance at which the theoretical variogram curve reaches its maximum is called the range (φ). The concept of practical range can be applied to models with an infinite range of values. The practical range is the distance at which the variogram reaches 95% of the asymptote. The practical threshold depends on the parameter τ^2, σ^2 and φ, respectively, where the latter is usually multiplied by a model-dependent constant. For example, the practical range is 3φ for the exponential model, √3φ for the Gaussian model, 4φ and 5φ for the Mathern model with κ = 1 and 2, respectively, and equal to φ for the spherical model (Diggle et al., 2003).

Spherical, exponential and Gaussian are the most commonly used variogram models. However, they lack the flexibility to account for a wider range of spatial patterns (Stein, 1999). The Matern variogram can be considered as an alternative to the common models (Minasny & McBratney, 2005b). Matern models are highly flexible for modelling the spatial covariance and are able to account for a wide range of local spatial processes. Therefore, the Matern model is proposed to be used as a general approach for modelling soil properties (Minasny & McBratney, 2005a) and environmental processes (Zhukov et al., 2021). The Matern isotropic covariance function has the form (Handcock & Stein, 1993; Stein, 1999):

$$F(h) = \frac{1}{2^{\kappa-1}\Gamma(\kappa)}\left(\frac{h}{\varphi}\right)^{\kappa} K_{\nu}\left(\frac{h}{\varphi}\right),$$

where h is the spacing distance; $K\nu$ is a modified Bessel function of second order κ; Γ is a gamma function; φ is a range or distance parameter (φ > 0), measuring the rate at which correlation decays with distance; κ is a smoothing parameter. The Matern model is highly flexible compared to the conventional geostatistical models due to the smoothing parameter κ. When the parameter κ is small ($\kappa \to 0$) the model describes a rough spatial process (Zimmermann et al., 2008). A rough spatial process corresponds to rapid changes in a feature at small distances (Minasny & McBratney, 2007). If the parameter κ is large ($\kappa \to \infty$), the model describes a smoothed spatial process (Minasny & McBratney, 2005a). The Matern model is fully consistent with the exponential model when $\kappa = 0.5$. The Matern model is fully consistent with the Gaussian model as $\kappa \to \infty$. The Matern model corresponds to the Whittle function if $\kappa = 1$ (Whittle, 1954; Webster, 2001). The spatial process is approximated by a power function if the range parameter r is large ($r \to \infty$), if $\kappa > 0$. The spatial process is modelled by a log function or a Wijs function if $\kappa \to 0$ (de Wijs, 1951, 1953). The ratio of nuggets to sill (spatial dependance level or SDL, %) was considered as an indicator of the strength of spatial autocorrelation. A variable is considered to have a strong spatial dependence if the SDL is less than 25%, and to have a moderate spatial dependence if the SDL is between 25% and 75%; otherwise, the variable has a weak spatial dependence (Sun et al., 2003).

Regression kriging. A spatial process can be the result of spatial autocorrelation and the effect of a total trend (Han et al., 2023). The spatial autocorrelation is considered as a result of the internal interaction of the phenomenon or process being modeled (Teng et al., 2018). The autocorrelation as a consequence of interaction decays with the distance between points in space, as the strength of the interaction that causes autocorrelation also decreases. Kriging is an adequate technique to model the spatial processes resulting from the spatial autocorrelation (Hoffman et al., 2023). A total spatial trend is the result of an external total force that regularly varies depending on the geographical coordinates. Therefore, the coordinates can be used as predictors in the regression analysis to explain the spatial variability of a feature under the influence of the total trend. Depending on the complexity of the spatial pattern undergone by the spatial process, the total trend can be described by a polynomial of the first, second, third, or higher orders. The real phenomena change in space under the influence of both external and internal causes. Therefore, regression kriging is used to model complex cases. Rgression kriging (RK) is a method of spatial interpolation that combines the regression of dependent variables on predictors with kriging of the forecast residuals (Hengl et al., 2004). The following equation calculates the regression kriging interpolation:

$$Z^*(x_0) = \hat{m}(x_0) + \hat{e}(x_0),$$

where $m(x_0)$ is the fitted deterministic part and $e(x_0)$ is the interpolated residual. Thus, the first part of the right-hand side of the equation represents the regression, and the second part represents the residual kriging. Calculations were performed using the geoR library(Ribeiro & Diggle, 2016).

Map accuracy, cross-validation, ME, NRMSE and MSDR. A cross-validation procedure was applied to assess the accuracy of the spatial models. Normalized root mean square error (NRMSE), mean error (ME), and mean square deviation ratio (MSDR) were calculated as statistics of the adequacy of the spatial models (Vasat et al., 2013). Root mean square error (RMSE) was calculated as follows:

$$RMSE = \sqrt{\frac{\sum_{i=1}^{n}(x_{1,i}-x_{2,i})^2}{n}}.$$

The normalized root mean square error (NRMSE) was calculated as follows:

$$NRMSE = \frac{RMSE}{x_{1,max}-x_{1,min}}.$$

The mean square deviation ratio (MSDR) was calculated as follows:

$$MSDR = \frac{\sum_{i=1}^{n}\left[\frac{(x_{1,i}-x_{2,i})^2}{var_i}\right]}{n}.$$

where x1 is the spatial prediction of the variable X; x_2 is the measurement of this variable; n is the number of observations; var is the kriging variance. The more accurate the spatial model, the lower the NRMSE value. The Mean Squared Deviation Ratio (MSDR) exhibits the degree to which the variance of the measurement data is replicated by the Kriging interpolation and ideally equals 1 (Vasat et al., 2013). The R^2 of the regression between the observed and predicted values following cross-validation is used due to its intuitive nature. The cross-validation procedure used the xvalid function from the geoR library (Ribeiro & Diggle, 2016).

Multinomial modeling of beta-diversity dynamics of plant communities. The parametric multinomial modeling (MDM) allows us to reflect variations in the beta-diversity of communities under the influence of complex environmental factors using the theory of General Linear Models, which is the basis to assess the changes in ecosystem diversity in time and space and to identify the important environmental factors that cause the dynamics of beta-diversity in the space or time (De'Ath, 2012). The Shannon entropy H was used to estimate the diversity of D:

$$H = -\sum_{i=1}^{S} p_i \ln p_i, \quad D = \exp(H),$$

where H is Shannon's entropy, D is Shannon's diversity, pi is the proportion of the i-th species in the community, S is the number of species in the community.

The diversity of a community can be summarized in terms of α-, β-, and γ-diversity (Gavish et al., 2019). For a collection of N sites, the α-entropy Hα is the arithmetic mean of the entropies of the individual sites:

$$H_\alpha = -\frac{\sum_{j=1}^{N}\sum_{i=1}^{S} p_{ij} \ln p_{ij}}{N},$$

where p_{ij} is the proportion of the i-th species in the j-th site.

Accordingly, the α-diversity of D, or Dα, is equal to the average geometric diversity of sites.

Hγ is the entropy calculated on the basis of the average proportions of species across sites:

$$H_\gamma = -\sum_{i=1}^{S} p_i \ln p_i = -\frac{\sum_{j=1}^{N}\sum_{i=1}^{S} p_{ij} \ln p_i}{N},$$

where p_i is the average proportion of the i-th species across N sites. Accordingly, γ-diversity can be estimated as Dγ = exp(Hγ).

The turnover of species between sites, or β-diversity, can be defined as (Jost, 2007):

$D_\beta = D_\gamma / D_\alpha$ and it follows that $H_\beta = H_\gamma - H_\alpha$.

The effect of single predictors or sets of predictors can be quantified for entropy, converted to diversity indices, and interpreted as the effective number of species. MDM is an extremely efficient and effective tool for the analysis of diversity. It is also structured in the same way as the aspect of nature it models. The environmental factors directly affect species and diversity changes as a result of these impacts. This process is reflected in MDM by modeling changes in the proportional abundance of species under the influence of environmental factors, and these changes are translated into diversity (De'Ath, 2012). MDM consists of three components: (I) the definition of parametric entropy (H), and parametric diversity (D). The H has a scale of computation that is additive. The D has a computational scale that expresses results as effective number of species, and is multiplicative. (2) A multinomial model (MM) that estimates the relationship established between proportional abundance and predictors. (3) The relationship between H and the MM log-likelihood function that provides the best estimates of proportional abundance for any given predictors, while minimizing H and D (De'Ath, 2012).

Results

Phytoindication of the impact of reconstruction on soil properties. The factor of park reconstruction and differences between polygons had a statistically significant effect on phytoindication assessments of ecological regimes ($F = 189.5$, $P < 0.001$ and $F = 34.2$, $P < 0.001$, respectively). These factors were able to explain 4.5% of the variation in the edaphotope moisture index ($F = 7.7$, $P < 0.001$). The moisture level assessed by phytoindication was significantly higher in the absence of reconstruction (11.41 ± 0.03) than in the park reconstruction (11.14 ± 0.05, Fig. 1). The variability between polygons was not a statistically significant cause of variation in edaphic moisture ($F = 0.3$, $P = 0.75$). The reconstruction and the differences between polygons were able to explain 57.3% of the variation in the index of variability of edaphic moisture ($F = 188.9$, $P < 0.001$). The level of variability of the moisture regime, which was assessed by phytoindication, was significantly higher under the conditions of reconstruction (5.61 ± 0.04) than within the park territory without reconstruction (4.33 ± 0.04). The variability between polygons was a statistically significant cause of the variation in edaphic moisture ($F = 14.4$, $P < 0.001$), but the contribution of this factor to the variability was much smaller than that of the reconstruction factor (5.5% vs. 51.8%). The reconstruction and differences between polygons were able to explain 56.8% of the variation in the acidity index of the edaphotope ($F = 184.6$, $P < 0.001$). The level of acidity of the edaphotope, assessed by phytoindication, was significantly higher under the conditions of reconstruction (9.09 ± 0.04) than within the park without reconstruction (7.96 ± 0.04). The variability between the polygons was a statistically significant cause of the variation in the acidity of the edaphic zone ($F = 39.3$, $P < 0.001$), but the contribution of this factor to variability was much smaller than that of the reconstruction factor (15.8% vs. 40.9%). The reconstruction and the differences between the polygons were able to explain 2.7% of the variation in the salinity index of the edaphotope ($F = 4.8$, $P = 0.002$). The level of salinity of the edaphotope, which was assessed by phytoindication, was slightly lower under the conditions of reconstruction (5.37 ± 0.02) than within the park territory without reconstruction (5.42 ± 0.02). The variability between the test polygons was a statistically significant cause of the variation in salinity ($F = 3.7$, $P = 0.024$) and the contribution of this factor to the variability was significantly greater than that of the reconstruction factor (0.2% vs. 2.5%). The reconstruction and the differences between the polygons were able to explain 66.8% of the variation in the carbonate index ($F = 282.0$, $P < 0.001$). The carbonate content estimated by phytoindication was higher under the conditions of reconstruction (6.63 ± 0.04) than within the park without reconstruction (5.41 ± 0.05). The variability between sites was a

statistically significant cause of the variation in carbonate content (F = 95.3, P < 0.001), but the contribution of this factor to the variability was slightly less than that of the reconstruction factor (29.9% vs. 36.8%). The reconstruction and the differences between the polygons were able to explain 44.0% of the variation in the nitrogen index (F = 110.5, P < 0.001). The nitrogen content estimated by phytoindication was higher under the conditions of reconstruction (9.42 ± 0.04) than within the park without reconstruction (8.55 ± 0.05). The variability between polygons was a statistically significant cause of the variation in nitrogen content (F = 13.2, P < 0.001), but the contribution of this factor to the variability was much smaller than that of the reconstruction factor (6.5% vs. 37.5%). The reconstruction and differences between the polygons were able to explain 54.2% of the variation in the aeration index (F = 166.4, P < 0.001). Soil aeration assessed by phytoindication was higher in the reconstructed area (7.40 ± 0.05) than in the unreconstructed area (6.00 ± 0.06). The variability between polygons was a statistically significant cause of the variation in aeration variability (F = 49.1, P < 0.001), but the contribution of this factor to the variability was slightly less than that of the reconstruction factor (21.1% vs. 33.1%). The reconstruction and differences between polygons were able to explain 54.2% of the variation in the aeration index (F = 166.4, P < 0.001). The soil aeration assessed by phytoindication was higher under the conditions of reconstruction (7.40 ± 0.05) than within the park area without reconstruction (6.00 ± 0.06). The variability between polygons was a statistically significant cause of the variation in aeration variability (F = 49.1, P < 0.001)but the contribution of this factor to the variability was somewhat smaller than that of the reconstruction factor (21.1% vs. 33.1%).

Phytoindication of the impact of reconstruction on climatic regimes. The climate scales also demonstrated the response of ecological regimes in the park in response to the reconstruction (Fig. 2). The reconstruction and differences between the polygons were able to explain 58.9% of the variation in the thermal regime index (F = 166.4, P < 0.001). The thermal regime assessed by phytoindication was lower under the conditions of reconstruction (9.31 ± 0.05) than within the park without reconstruction (10.01 ± 0.08). The variability between the test polygons was a statistically significant cause of the variation in thermal regime variability (F = 244.6, P < 0.001) and the contribution of this factor to variability was exclusive. The reconstruction and the differences between the polygons were able to explain 56.1% of the variation in the ombroclimate index (F = 166.4, P < 0.001). Ombroclimate, assessed by phytoindicators, was higher under the restoration conditions (14.32 ± 0.06) than in the park without restoration (13.16 ± 0.07). The variation between the locations was a statistically significant contributor to the alteration in ombroclimate variability (F = 135.0, P < 0.001) and the contribution of this factor to variability was exclusive. The reconstruction and the differences between the polygons were able to explain 32.9% of the variation in the continentality index (F = 69.5, P < 0.001). The continentality index estimated by phytoindication was higher in the reconstructed area (6.60 ± 0.07) than in the unreconstructed area (5.61 ± 0.07). The variability between polygons was a statistically significant cause of the variation in continentality (F = 56.2, P < 0.001) and the contribution of this factor to variability was exceptional. The reconstruction and differences between the polygons were able to explain 14.8% of the variation in the cryoclimate index (F = 25.3, P < 0.001). The reconstruction conditions resulted in a higher cryoclimate index, assessed by phytoindication (10.20 ± 0.05), than within the park without reconstruction (9.79 ± 0.03). The variability between the polygons was a statistically significant cause of the variation in cryoclimate variability (F = 15.0, P < 0.001) and the contribution of this factor to the variability was more significant (11.5%) than that of the reconstruction factor (3.3%). The reconstruction and the differences between the polygons were able to explain 76.1% of the variation in the light index (F = 76.1, P < 0.001). The light index estimated by phytoindication was higher under the conditions of reconstruction (7.44 ± 0.04) than within the park area without reconstruction (5.34 ± 0.07). The variability between polygons was a statistically significant cause of the variation in light variability (F = 109.3, P < 0.001) but the contribution of this factor to the variability was much smaller (24.7%) than the contribution of the reconstruction factor (51.4%).

Spatial variation of phytoindication evaluations of environmental factors. The assessment of spatial variability and geostatistics allows us to identify the causes of variation in the attributes related to spatial factors. The phytoindication assessment of the productive moisture content in the soil indicates a level of 99–103 mm. This level of moisture can be recognized as satisfactory. The spatial variation of phytoindication estimates of soil moisture content was much more spatially structured as a result of reconstruction than without reconstruction, as evidenced by the lower values of the SDL index for the spatial models of the reconstructed polygons a and b (7.1% and 30.6%) and for the unreconstructed polygons c and d (38.8% and 64.2%, Fig. 3). The typical size of the spatial structures of phytoindication estimates of soil moisture decreased as a result of reconstruction, as evidenced by the reduction of the practical range. This parameter was 5.3 and 7.4 meters for polygons a and b, respectively, and 8.1 and 24.5 meters for polygons c and d, respectively. The Kappa parameter indicates the similarity of spatial models that can be used to display spatial patterns both with and without reconstruction.

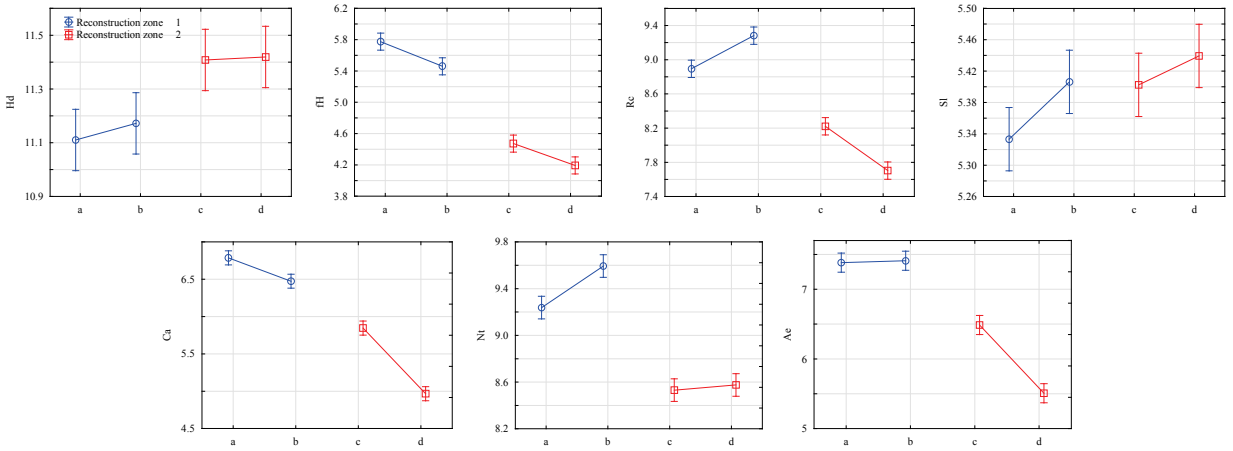

Fig. 1. The dependence of phytoindication assessments of soil regimes on the impact of park reconstruction: the mean value ± 0.95 confidence interval (N = 105) is presented; the abscissa axis is the polygons (*a*, *b*, *c*, *d*), and the ordinate axis represents the phytoindication scores: Hd is the soil water regime; fH is the variability of damping, Rc is the soil acidity, Sl is the total salt regime, Ca is the carbonate content in soil, Nt is the nitrogen content in soil, Ae is the soil aeration; the variable "Park reconstruction" has two states: "Reconstruction Zone 1" is the territory where reconstruction processes took place (polygons a and b), and "Reconstruction Zone 2" is the territory where no park reconstruction processes took place (polygons c and d)

The phytoindication assessment of the coefficient of moisture unevenness ω shows that under the conditions of reconstruction it was equal to 0.20–0.21, which indicates conditions favorable for hemihydrocontrastophobes. The coefficient ω was equal to 0.14–0.15 under conditions without reconstruction, indicating an environment favorable to hydrocontrastophobes. Thus, the reconstruction resulted in an increase in moisture contrast conditions. The spatial patterns of variability of edaphic moisture had a lower level of the practical range under the reconstruction process

than without reconstruction (Fig. 4). The Kappa parameter was higher for the reconstruction conditions. This parameter was 7.5 and 7.0 for sites a and b, respectively, and 1 and 5 for sites c and d, respectively. The phytoindication assessment of pH under the conditions of reconstruction resulted in values of 6.82–6.91, and under the conditions without reconstruction it was 6.51–6.82. The spatial structuredness of the variation of the phytoindication indicator of soil acidity was less for the conditions after reconstruction (for polygons a and b, the SDL indicator was 58.3 and 12.9%, respectively) than for the conditions without reconstruction (for polygons c and d, the SDL indicator was 6.5 and 28.7%, respectively) (Fig. 5). Both the practical range and the Kappa value did not demonstrate features specific to the impact of reconstruction on the spatial patterns of soil acidity.

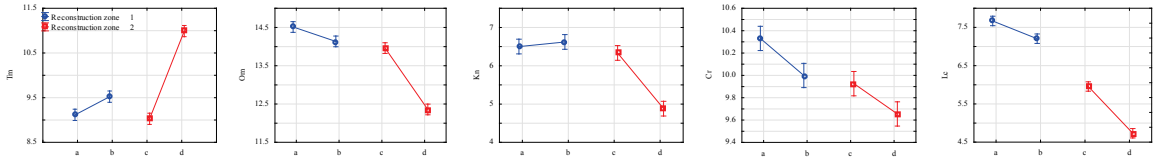

Fig. 2. The dependence of phytoindication assessments of climatic regimes on the impact of park reconstruction: the mean value ± 0.95 confidence interval (N = 105) is presented; the abscissa axis is the polygons (a, b, c, d), the ordinate axis represents the phytoindication estimates: Tm is the thermal climate, Om is the humidity, Kn is the continentality of climate, Cr is the cryoregime of climate, Lc is the light regime; the variable "Park reconstruction" has two states: "Reconstruction Zone 1" is the territory where reconstruction processes took place (polygons a and b), and "Reconstruction Zone 2" is the territory where no park reconstruction processes took place (polygons c and d)

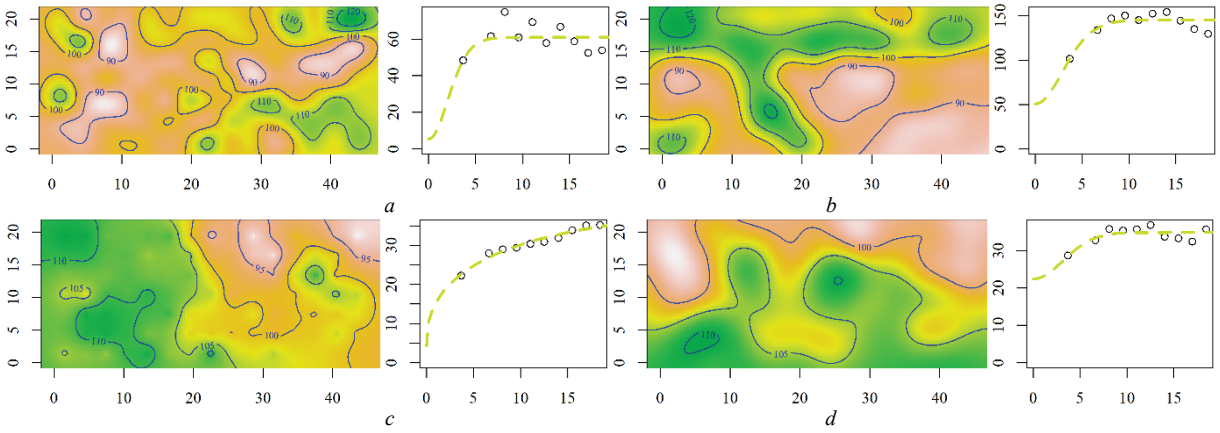

Fig. 3. The spatial variation of the phytoindication assessment of the soil moisture regime and the variogram of the spatial model: the isoline indicates the value of productive moisture content in a meter layer (mm); the spatial model is shown in local coordinates; the abscissa and ordinate axes are given in meters; the abscissa axis of the variogram is the distance (m); the ordinate axis is the variation; polygon a: Mean = 99.57 ± 63.7, Phi = 0.48, Practical range = 5.36, Sill = 56.65, Nugget = 4.3, SDL = 7.05, Kappa = 10, R^2 of trend = 0.12, NRMSE = 0.14, ME*10^{-3} = 83.26, MSDR = 0.97, R^2 of cross validation = 0.11; polygon b: Mean = 100.28 ± 131.36, Phi = 0.66, Practical range = 7.39, Sill = 100.78, Nugget = 44.39, SDL = 30.58, Kappa = 10, R^2 of trend = 0.23, NRMSE = 0.11, ME*10^{-3} = –6.8, MSDR = 0.64, R^2 of cross validation = 0.35; polygon c: Mean = 103.42 ± 61.44, Phi = 8.19, Practical range = 24.52, Sill = 22.57, Nugget = 14.35, SDL = 38.87, Kappa = 0.5, R^2 of trend = 0.35, NRMSE = 0.14, ME*10^{-3} = –13.27, MSDR = 0.76, R^2 of cross validation = 0.23; polygon d: Mean = 103.39 ± 76.72, Phi = 0.73, Practical range = 8.14, Sill = 12.48, Nugget = 22.42, SDL = 64.24, Kappa = 10, R^2 of trend = 0.14, NRMSE = 0.22, ME*10^{-3} = –11.14, MSDR = 0.86, R^2 of cross validation = 0.14

The phytoindication assessment indicates the soil solution contained 18.37–19.27 μg/L of salts. This level is favorable for semieutrophs. The reconstruction did not affect the overall level of salt content, but the spatial structure of soil salinity variability decreased under the influence of reconstruction, as indicated by higher SDL values (Fig. 6). The practical range of spatial models of soil salinity variability under the influence of reconstruction stabilized and was within narrower limits (8.6–9.6 meters) than without reconstruction (4.6–17.8 meters). The Kappa parameter indicates the similarity of spatial patterns of soil salinity, which can be used to reflect the spatial patterns both under conditions of reconstruction and without it.

The phytoindication assessment of carbonate content under reconstruction conditions indicates the presence of 1.31–1.58%, which indicates an environment favorable to acarbonatophiles. The carbonate content was 0.45–0.88% under conditions without reconstruction, favorable for hemicarbonatophiles. The spatial structure of the variability of carbonate content in the soil also decreased under the influence of reconstruction, as indicated by higher SDL values (Fig. 7). This indicator was 48.4% and 55.8% for polygons a and b, respectively, and 27.2% and 6.7 % for polygons c and d, respectively. The spatial structures of the patterns of calcium content variability decreased under the conditions of reconstruction, as evidenced by the value of the practical range. The Kappa values indicated heterogeneous spatial models that are most suitable for describing spatial processes under reconstruction conditions compared to conditions without reconstruction.

The phytoindication assessment indicates that the plant community after reconstruction had an optimal nitrogen content of 4.5–4.6 g/kg, which created favorable conditions for eunitrophiles. The optimal nitrogen content in the soil without reconstruction was 4.43–4.44 g/kg, which was favorable for nitrophiles. The spatial structure of the variation of nitrogen content in the soil did not depend on the influence of reconstruction (Fig. 8). The practical range of variation in nitrogen content decreased under the influence of reconstruction. The Kappa values indicated the homogeneous spatial models that are most suitable for describing spatial processes under the reconstruction conditions compared to the conditions without reconstruction.

The optimal aeration regime for the plant community after reconstruction was 37.2–37.4% of the pore space volume. These conditions are favorable for hemiaerophobes. The optimal conditions for the plant community without reconstruction were the aeration regime of 49.4–64.6% of the pore space volume. These conditions were favorable for subaerophiles. The spatial structure of the variability of phytoindication assessments of soil aeration did not depend on the impact of reconstruction, but was significantly dependent on the characteristics of a particular polygon. The spatial variation of soil aeration under the influence of reconstruction acquires features under which the practical range is largely stabilized, while without reconstruction this indicator is largely variable (Fig. 9). The Kappa values also showed a significant dependence on the characteristics of a particular test site. The spatial patterns of variability of soil aeration are quite different between the polygons, which makes it impossible to reveal the likely impact of the park reconstruction on this indicator.

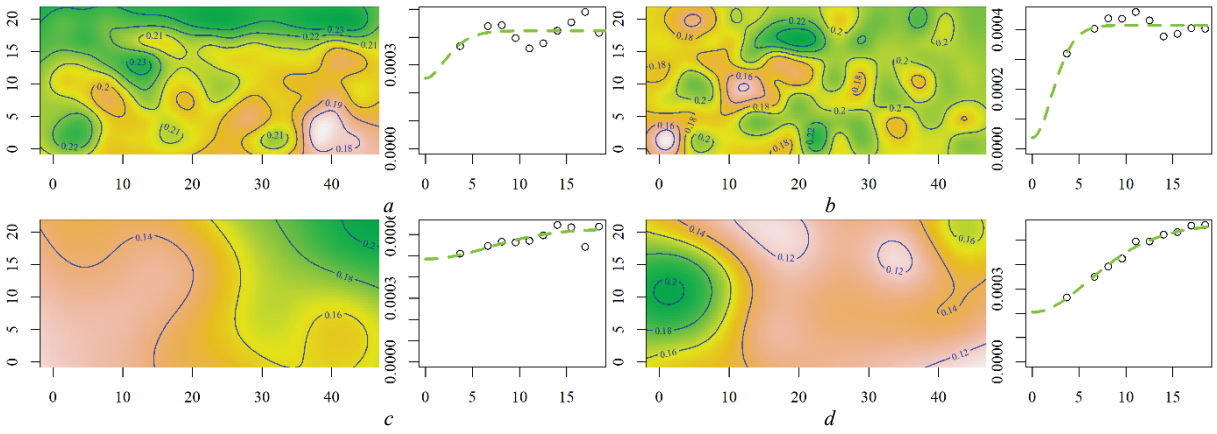

Fig. 4. The spatial variation of the phytoindication assessment of soil moisture regime variability and the variogram of the spatial model: the isoline indicates the value of the phytoindication assessment; the spatial model is shown in local coordinates; the abscissa and ordinate axes are given in meters; the abscissa axis of the variogram is the distance (m); the ordinate axis is the variation; polygon a: Mean = 0.21 ± 62.94, Phi = 0.7, Practical range = 6.88, Sill = 0.00016, Nugget = 0.00027, SDL = 62.94, Kappa = 7.5, R^2 of trend = 0.18, NRMSE = 0.19, ME*10^{-3} = 0.1, MSDR = 0.81, R^2 of cross validation = 0.22; polygon b: Mean = 0.2 ± 6.24, Phi = 0.6, Practical range = 5.68, Sill = 0.0004, Nugget = 0, SDL = 6.24, Kappa = 7, R^2 of trend = 0.14, NRMSE = 0.12, ME*10^{-3} = –0.09, MSDR = 0.83, R^2 of cross validation = 0.19; polygon c: Mean = 0.15 ± 52.58, Phi = 2.4, Practical range = 9.6, Sill = 0.00029, Nugget = 0.00032, SDL = 52.58, Kappa = 1, R^2 of trend = 0.29, NRMSE = 0.16, ME*10^{-3} = 0.09, MSDR = 0.9, R^2 of cross validation = 0.09; Polygon d: Mean = 0.14 ± 36.54, Phi = 2.4, Practical range = 19.42, Sill = 0.00037, Nugget = 0.00021, SDL = 36.54, Kappa = 5, R^2 of trend = 0.19, NRMSE = 0.13, ME*10^{-3} = –0.07, MSDR = 0.47, R^2 of cross validation = 0.52

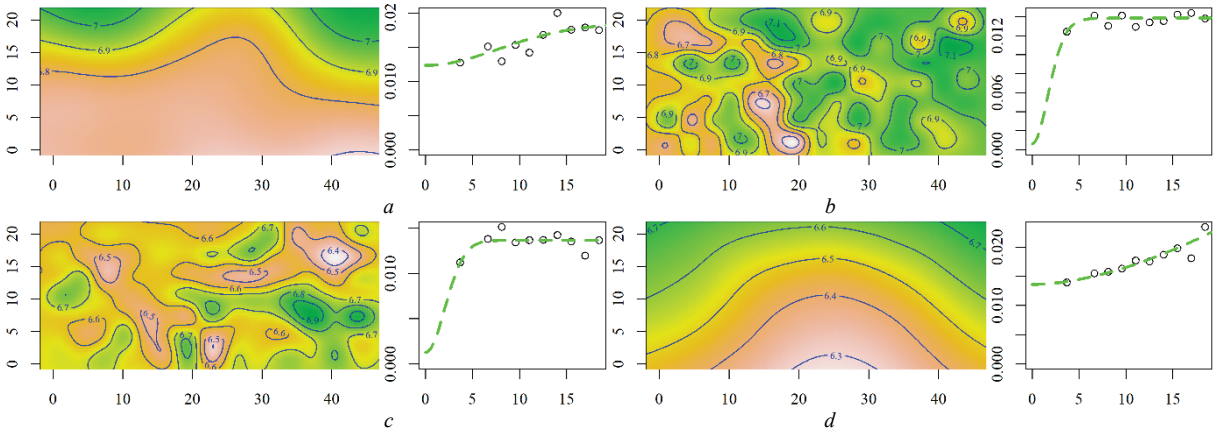

Fig. 5. The spatial variation of the phytoindication assessment of the soil acidity regime and the variogram of the spatial model: the isoline indicates the soil pH value; the spatial model is shown in local coordinates; the abscissa and ordinate axes are in meters; the abscissa axis of the variogram is the distance (m); the ordinate axis is the variation; polygon a: Mean = 6.82 ± 58.38, Phi = 4.23, Practical range = 20.05, Sill = 0.01, Nugget = 0.01, SDL = 58.37, Kappa = 1.5, R^2 of trend = 0.22, NRMSE = 0.2, ME*10^{-3} = 0.46, MSDR = 0.9, R^2 of cross validation = 0.09; polygon b: Mean = 6.91 ± 12.95, Phi = 0.41, Practical range = 4.47, Sill = 0.0121, Nugget = 0.0018, SDL = 12.94, Kappa = 9.5, R^2 of trend = 0.26, NRMSE = 0.14, ME*10^{-3} = –0.25, MSDR = 0.96, R^2 of cross validation = 0.05; polygon c: Mean = 6.64 ± 6.46, Phi = 0.47, Practical range = 5.11, Sill = 0.01279, Nugget = 0.00088, SDL = 6.45, Kappa = 9.5, R^2 of trend = 0.07, NRMSE = 0.14, ME*10^{-3} = 0.39, MSDR = 0.91, R^2 of cross validation = 0.13; polygon d: Mean = 6.51 ± 28.74, Phi = 24.88, Practical range = 99.5, Sill = 0.03156, Nugget = 0.012, SDL = 28.71, Kappa = 1, R^2 of trend = 0.25, NRMSE = 0.18, ME*10^{-3} = 0.12, MSDR = 0.78, R^2 of cross validation = 0.21

A plant community was formed in the park planting, for which the optimal radiation balance is 1.8–2.3 gJ/m^2 year. Such conditions are favorable for submesotherms of nemoral/sub-Mediterranean climate. The variation of the phytoindicator assessment of the thermal climate was either very spatially dependent (SDL equal to 0.1% or 6.4%) or moderately spatially dependent (SDL equal to 41.5% or 63.5%), but this variation in the level of spatial dependence could not be attributed to the impact of the park reconstruction (Fig. 10). The reconstruction led to changes in spatial variation in such a way that spatial structures of smaller extent were formed, as evidenced by a smaller value of the practical range (4.3–8.4 meters), while in areas of the park without reconstruction the practical range was much larger (12.1–48.6 meters). The spatial model was used to describe the best thermal climate under the conditions of reconstruction, which had a Kappa of 9.0–9.5. For the spatial process without reconstruction, the best models were those with Kappa equal to 0.5–2.0.

These conditions were favorable for mesoombrophytes. For the conditions without reconstruction, this indicator was –0.31–0.55 mm, indicating conditions that were favorable for subombrophytes. The spatial variation of the phytoindication assessment of the ombroclimate was moderately spatially dependent, as evidenced by the SDL in the range of 51.9–67.5% (Fig. 11). Also, the practical range did not differ between the sites depending on the impact of reconstruction. The spatial patterns under reconstruction conditions could be best described by a variogram with Kappa equal to 1.5, while under conditions without reconstruction Kappa was 0.5 and 3.0.

The phytoindication assessment of the continental regime under the reconstruction conditions was 106.08–106.72, and under the conditions without reconstruction this indicator was 90.06–104.25. These results indicate an environment typical of the hemi-oceanic climate. The variation in the phytoindication score of continentality was strongly or moderately spatially dependent, but the spatial dependence was not influenced by the park reconstruction factor (Fig. 12). The practical range of the spatial process under reconstruction conditions had a slightly smaller spatial range. The differences in the Kappa parameter cannot be attributed to the influence of the reconstruction factor.

The phytoindication assessment of the average temperature of the coldest month of the year indicates 0.18–1.64 °C for the conditions after

reconstruction and –1.12 – –0.16 °C for the conditions before reconstruction. The variation of the phytoindication assessment of the cryoclimate was moderately spatially dependent, as evidenced by the SDL value in the range of 63.5–68.9% (Fig. 13). The spatial dependence of the cryoclimate was not affected by the reconstruction. Also, the variability of the spatial range cannot be explained by the influence of reconstruction. The Kappa values indicate the homogeneity of spatial models that can explain the spatial variation of the cryoclimate.

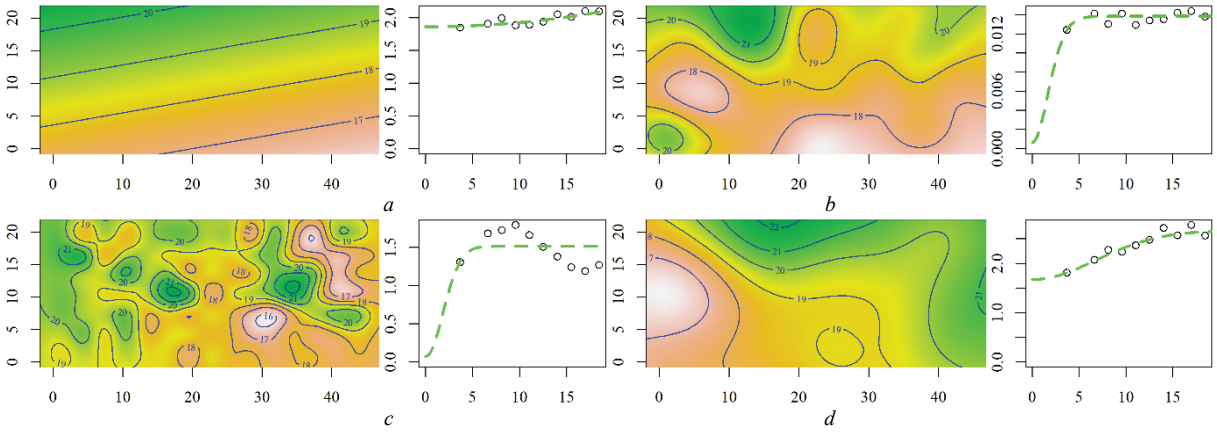

Fig. 6. The spatial variation of the phytoindication assessment of soil salinity regime and the variogram of the spatial model: the isoline indicates the content of soluble salts in the soil solution (μg/L); the spatial model is shown in local coordinates; the abscissa and ordinate axes are in meters; the abscissa axis of the variogram is the distance (m); the ordinate axis is the variation; polygon a: Mean = 18.37 ± 63.98, Phi = 2.87, Practical range = 8.58, Sill = 0.73, Nugget = 1.26, SDL = 63.25, Kappa = 0.5, R^2 of trend = 0.29, NRMSE = 0.19, ME*10^{-3} = –0.24, MSDR = 0.99, R^2 of cross validation = 0.01; polygon b: Mean = 18.95 ± 61.3, Phi = 0.86, Practical range = 9.65, Sill = 0.83, Nugget = 1.26, SDL = 60.47, Kappa = 10, R^2 of trend = 0.16, NRMSE = 0.19, ME*10^{-3} = 4.72, MSDR = 0.86, R^2 of cross validation = 0.13; polygon c: Mean = 18.92 ± 7.77, Phi = 0.41, Practical range = 4.65, Sill = 1.42, Nugget = 0.1, SDL = 6.35, Kappa = 10, R^2 of trend = 0.2, NRMSE = 0.11, ME*10^{-3} = 0.65, MSDR = 0.81, R^2 of cross validation = 0.18; polygon d: Mean = 19.27 ± 63.12, Phi = 1.59, Practical range = 17.78, Sill = 1.02, Nugget = 1.67, SDL = 62.1, Kappa = 10, R^2 of trend = 0.27, NRMSE = 0.14, ME*10^{-3} = 4.16, MSDR = 0.76, R^2 of cross validation = 0.23

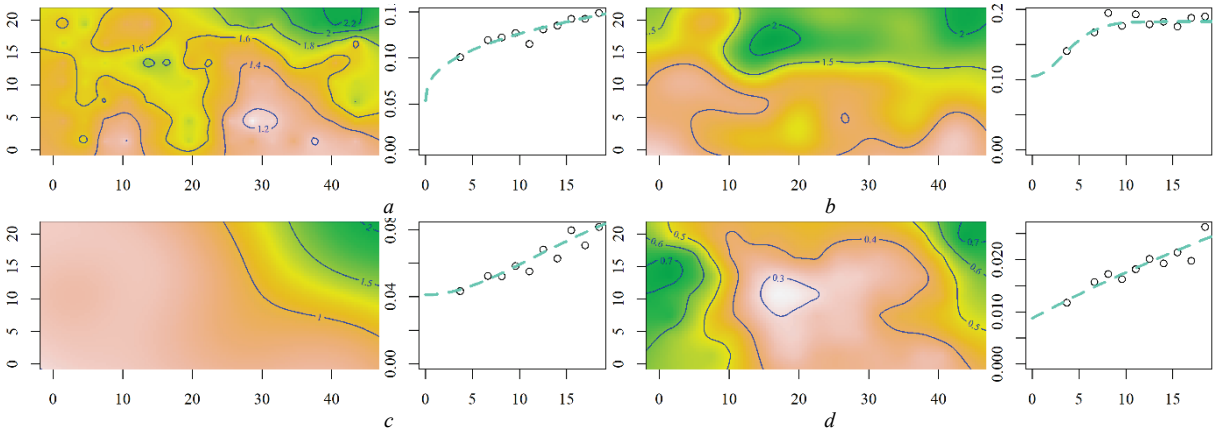

Fig. 7. The spatial variation of phytoindication assessment of carbonate content in soil and the variogram of the spatial model: the isoline indicates the content of carbonates in the soil, CaO and MgO (%); the spatial model is shown in local coordinates; the abscissa and ordinate axes are in meters; the abscissa axis of the variogram is the distance (m); the ordinate axis is the variation; polygon a: Mean = 1.58 ± 48.51, Phi = 13.78, Practical range = 41.28, Sill = 0.09, Nugget = 0.08, SDL = 48.42, Kappa = 0.5, R^2 of trend = 0.1, NRMSE = 0.27, ME*10^{-3} = 0.86, MSDR = 0.91, R^2 of cross validation = 0.08; polygon b: Mean = 1.31 ± 55.83, Phi = 0.78, Practical range = 8.48, Sill = 0.08, Nugget = 0.1, SDL = 55.75, Kappa = 9.5, R^2 of trend = 0.28, NRMSE = 0.14, ME*10^{-3} = –0.98, MSDR = 0.75, R^2 of cross validation = 0.24; polygon c: Mean = 0.88 ± 27.27, Phi = 17.45, Practical range = 69.76, Sill = 0.1, Nugget = 0.04, SDL = 27.17, Kappa = 1, R^2 of trend = 0.5, NRMSE = 0.09, ME*10^{-3} = 0.05, MSDR = 0.62, R^2 of cross validation = 0.38; polygon d: Mean = 0.45 ± 6.82, Phi = 149.69, Practical range = 448.42, Sill = 0.13, Nugget = 0.01, SDL = 6.69, Kappa = 0.5, R^2 of trend = 0.05, NRMSE = 0.18, ME*10^{-3} = 0.33, MSDR = 0.61, R^2 of cross validation = 0.39

The lighting regime under the reconstruction conditions was characterized by a score of 7.2–7.6, which corresponded to the regime of semi-open spaces. The light regime under conditions without reconstruction had a score of 4.7–5.9, which corresponded to the light forest regime. The spatial dependence of lighting under the conditions of reconstruction was moderate (SDL values were in the range of 51.8–54.8%), and under the conditions of no reconstruction, the spatial dependence was moderate or highly spatially dependent (SDL values were in the range of 13.3–36.1%, Fig. 14). The practical range under reconstruction conditions was much smaller (6.4–8.8 meters) than under conditions of no reconstruction (36.2–155.3 meters). The best model in the reconstruction condition was the one with Kappa equal to 10. The best model for the conditions without reconstruction was the one with Kappa equal to 0.5.

There was a statistically significant tendency for all spatial processes to decrease the practical range of the variogram under the influence of reconstruction (F = 4.42, P = 0.04). The practical range was usually 9.6 ± 1.6 meters under the conditions of reconstruction, and without reconstruction this figure was 46.1 ± 18.9 meters. The effect of reconstruction on the practical range did not depend on the phytoindication scale (F = 1.25, P = 0.31). The practical range did not differ between phytoindicator scales (F = 1.62, P = 0.16) except for the carbonate scale, for which the radius was larger than the others (Planned comparison F = 15.8, P < 0.001). The spatial dependence reflected by the SDL showed a downward trend under the influence of reconstruction, although this effect was not statistically significant in the traditional sense (F = 1.69, P = 0.08). The SDL was 43.4 ± 5.0% under reconstruction conditions, and 37.1 ± 5.0% under conditions without reconstruction. Differences between phytoindication

scales in terms of spatial dependence were not statistically significant (F = 0.92, P = 0.54). The reconstruction tended to increase Kappa for the best spatial model (F = 3.95, P = 0.05). The effect of reconstruction on the Kappa parameter did not depend on the phytoindication scale (F = 1.26, P = 0.30). The effect of reconstruction on the linear trend of variability of phytoindication scales was not statistically significant (F = 0.64, P = 0.85). Also, the quantitative characteristics of the quality of spatial models did not depend on the influence of reconstruction and phytoindication scale.

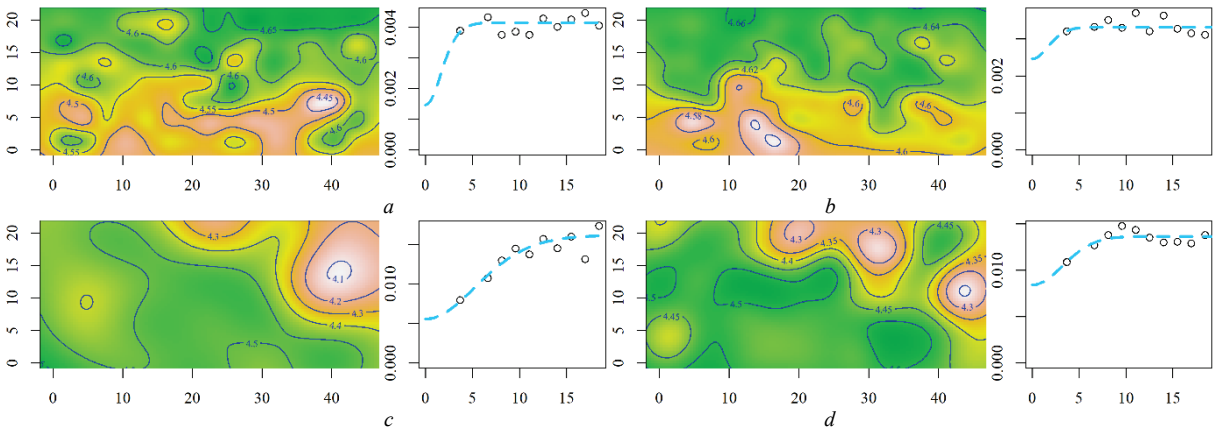

Fig. 8. The spatial variation of the phytoindication assessment of soil nitrogen content and the variogram of the spatial model: the isoline indicates the nitrogen content in the soil (g/kg); the spatial model is shown in local coordinates; the abscissa and ordinate axes are in meters; the abscissa axis of the variogram is the distance (m); the ordinate axis is the variation; polygon a: Mean = 4.57 ± 13.33, Phi = 0.41, Practical range = 4.55, Sill = 0.0036, Nugget = 0.001, SDL = 13.33, Kappa = 8, R^2 of trend = 0.27, NRMSE = 0.12, ME*10^{-3} = 0.01, MSDR = 0.92, R^2 of cross validation = 0.09; polygon b: Mean = 4.62 ± 64.57, Phi = 0.4, Practical range = 4.38, Sill = 0, Nugget = 0, SDL = 64.57, Kappa = 9.5, R^2 of trend = 0.1, NRMSE = 0.3, ME*10^{-3} = 0.01, MSDR = 0.98, R^2 of cross validation = 0.01; polygon c: Mean = 4.43 ± 35.90, Phi = 1.3, Practical range = 14.53, Sill = 0.01043, Nugget = 0.00584, SDL = 35.89, Kappa = 10, R^2 of trend = 0.28, NRMSE = 0.11, ME*10^{-3} = –0.09, MSDR = 0.5, R^2 of cross validation = 0.49; polygon d: Mean = 4.44 ± 53.12, Phi = 0.69, Practical range = 7.57, Sill = 0.00639, Nugget = 0.00724, SDL = 53.12, Kappa = 9.5, R^2 of trend = 0.09, NRMSE = 0.2, ME*10^{-3} = –0.39, MSDR = 0.82, R^2 of cross validation = 0.17

Principal component analysis of variation in phytoindication assessments of environmental factors. The principal component analysis of the variation in phytoindication scores of environmental factors identified three principal components with eigenvalues greater than one (Table 1). These three principal components together were able to explain 71.2% of the variation in phytoindication scores. The principal component 1 was able to explain 47.8% of the variation in phytoindication scores and indicated the variation in light conditions within the studied sites. This component indicated an increase in the variability of moisture, acidity, carbonate, nitrogen content, soil aeration, ombroclimate, continentality, and cryoclimate. The increase in lighting decreased the soil moisture and mineralization, as well as the assessment of the thermal climate. The park reconstruction factor was able to statistically significantly explain 54.2% of the variation in principal component 1 (F = 497.9, P < 0.001).

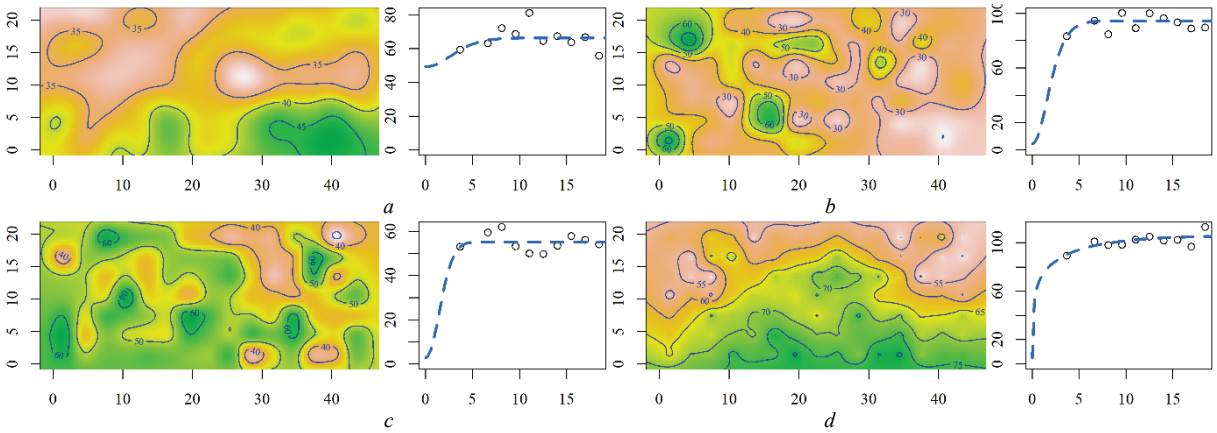

Fig. 9. The spatial variation of the phytoindication assessment of the soil aeration regime and the variogram of the spatial model: the isoline indicates the proportion of the soil vapor space occupied by air; the spatial model is shown in local coordinates; the abscissa and ordinate axes are in meters; the abscissa axis of the variogram is the distance (m); the ordinate axis is the variation; polygon a: Mean = 37.42 ± 89.32, Phi = 0.63, Practical range = 6.56, Sill = 21.05, Nugget = 45.3, SDL = 68.27, Kappa = 8.5, R^2 of trend = 0.09, NRMSE = 0.27, ME*10^{-3} = 11.43, MSDR = 0.94, R^2 of cross validation = 0.06; polygon b: Mean = 37.25 ± 94.77, Phi = 0.57, Practical range = 4.64, Sill = 88.17, Nugget = 6.23, SDL = 6.6, Kappa = 5, R^2 of trend = 0.23, NRMSE = 0.11, ME*10^{-3} = 12.95, MSDR = 0.77, R^2 of cross validation = 0.24; Polygon c: Mean = 49.42 ± 58.31, Phi = 0.32, Practical range = 3.59, Sill = 51.58, Nugget = 3.72, SDL = 6.73, Kappa = 10, R^2 of trend = 0.15, NRMSE = 0.13, ME*10^{-3} = –0.79, MSDR = 0.91, R^2 of cross validation = 0.11; polygon d: Mean = 64.55 ± 101.81, Phi = 4.48, Practical range = 13.41, Sill = 34.75, Nugget = 70.74, SDL = 67.06, Kappa = 0.5, R^2 of trend = 0.23, NRMSE = 0.22, ME*10^{-3} = –4.88, MSDR = 0.89, R^2 of cross validation = 0.1

The principal component 2 was able to explain 12.8% of the variation in phytoindicator scores and indicated the variation in soil moisture regime within the studied sites. This component indicated that with an increase in soil moisture, the index of ombroclimate, continental climate and cryoclimate increased. The increase in soil moisture decreased the variability of soil moisture and acidity, as well as nitrogen content, aeration, and thermal climate. The variability of light did not depend on this main component. The factor of park reconstruction did not affect the variation of principal component 2. The differences between sites were able to explain 33.0% of the variation in this principal component (F = 96.1, P < 0.001). The prin-

cipal component 3 was able to explain 10.6% of the variation in phytoindicator scores and indicated variation in soil mineralization within the studied sites. This component indicated that as soil mineralization increased, so did moisture, acidity, soil area, and continentality. With an increase in soil mineralization, the variability of moisture and ombroclimate decreased. The variability of light, carbonate and nitrogen content in the soil, and thermal climate did not depend on this main component. The factor of park reconstruction was not able to statistically significantly explain the variation in principal component 3 (F = 0.69. P = 0.40).

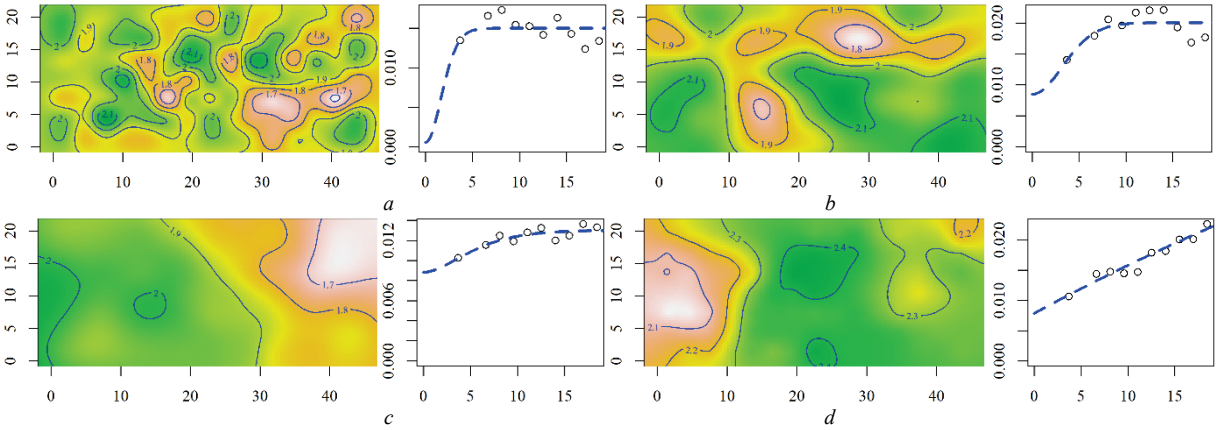

Fig. 10. The spatial variation of the phytoindication assessment of the thermal climate and the variogram of the spatial model: the isoline indicates the value of the radiation balance (gJ/m^2 year); the spatial model is shown in local coordinates; the abscissa and ordinate axes are in meters; the abscissa axis of the variogram is the distance (m); the ordinate axis is the variation; polygon a: Mean = 1.91 ± 6.37, Phi = 0.4, Practical range = 4.3, Sill = 0.01, Nugget = 0, SDL = 6.36, Kappa = 9, R^2 of trend = 0.07, NRMSE = 0.16, ME*10^{-3} = 0.07, MSDR = 0.94, R^2 of cross validation = 0.06; polygon b: Mean = 2.00 ± 41.49, Phi = 0.77, Practical range = 8.39, Sill = 0.01, Nugget = 0.01, SDL = 41.48, Kappa = 9.5, R^2 of trend = 0.09, NRMSE = 0.18, ME*10^{-3} = 0.67, MSDR = 0.67, R^2 of cross validation = 0.32; polygon c: Mean = 1.88 ± 63.53, Phi = 2.25, Practical range = 12.06, Sill = 0.00474, Nugget = 0.00825, SDL = 63.53, Kappa = 2, R^2 of trend = 0.35, NRMSE = 0.17, ME*10^{-3} = –0.29, MSDR = 0.91, R^2 of cross validation = 0.09; polygon d: Mean = 2.29 ± 115.76, Phi = 16.47, Practical range = 48.62, Sill = 115.75, Nugget = 0.01, SDL = 0.01, Kappa = 0.5, R^2 of trend = 0.14, NRMSE = 0.2, ME*10^{-3} = –0.21, MSDR = 0.7, R^2 of cross validation = 0.29

Spatial variability of plant community β-diversity under the influence of park reconstruction. The MDM analysis shows that the γ-diversity of the community was 16.6 and the α-diversity was 4.8 (Table 2). Accordingly, the γ-entropy was 2.81 and the α-entropy was 1.57. The difference between γ- and α-entropy was equal to β-entropy, which was 1.24. Species turnover, characterized by β-entropy, is induced by environmental factors, and the contribution to species turnover can be determined by MDM analysis. The influence of the principal components PC1, PC2, PC3 and the reconstruction factor, as well as the characteristics of the polygons, were statistically significant. The largest contribution to species turnover was made by PC1, which initiated 0.33 differentiation of entropy, or 26.6% of the total β-entropy. The contribution of reconstruction to species turnover was 0.15 entropy differentiation, or 12.1% of total β-entropy. Polygon features were responsible for 0.14 entropy differentiation, or 11.3% of the total β-entropy. The contribution of PC2 and PC3 was 0.08 and 0.04 entropy differentiation, or 6.5 and 3.2% of the total β-entropy, respectively. Unaccounted for factors provided 0.50 entropy differentiation, or 40.3% of the total β-entropy.

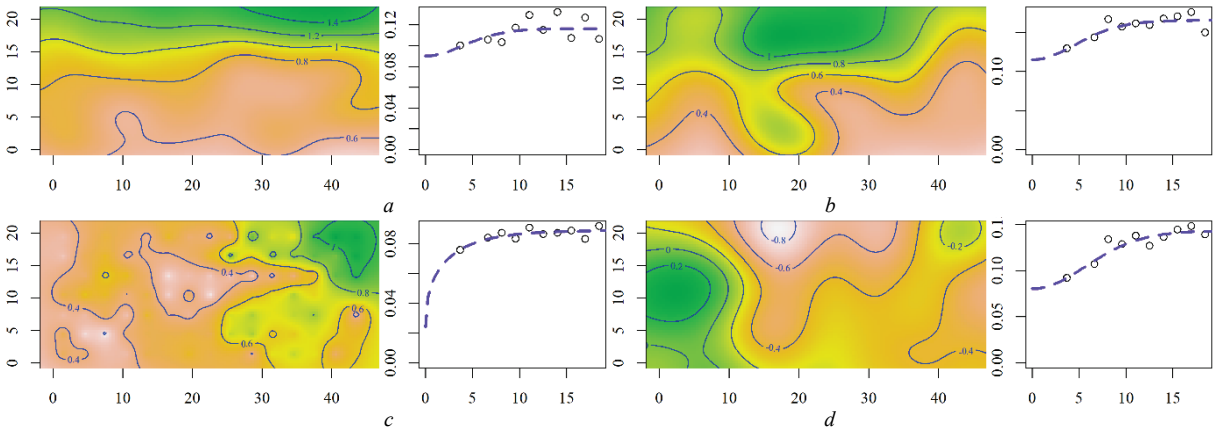

Fig. 11. The spatial variation of the phytoindication assessment of the ombroclimate and the variogram of the spatial model: the isoline indicates the difference between the average annual precipitation per day and evaporation from the open water surface for the same period (mm); the spatial model is shown in local coordinates; the abscissa and ordinate axes are in meters; the abscissa axis of the variogram is the distance (m); the ordinate axis is the variation; polygon a: Mean = 0.87 ± 67.57, Phi = 2.08, Practical range = 9.87, Sill = 0.04, Nugget = 0.08, SDL = 67.53, Kappa = 1.5, R^2 of trend = 0.27, NRMSE = 0.21, ME*10^{-3} = 1.67, MSDR = 0.9, R^2 of cross validation = 0.09; polygon b: Mean = 0.62 ± 60.65, Phi = 2.6, Practical range = 12.32, Sill = 0.07, Nugget = 0.1, SDL = 60.58, Kappa = 1.5, R^2 of trend = 0.19, NRMSE = 0.19, ME*10^{-3} = –1.57, MSDR = 0.82, R^2 of cross validation = 0.17; polygon c: Mean = 0.55 ± 57.41, Phi = 3.41, Practical range = 10.21, Sill = 0.04, Nugget = 0.05, SDL = 57.37, Kappa = 0.5, R^2 of trend = 0.18, NRMSE = 0.22, ME*10^{-3} = 0.14, MSDR = 0.93, R^2 of cross validation = 0.06; polygon d: Mean = –0.31 ± 51.92, Phi = 2.46, Practical range = 15.76, Sill = 0.07, Nugget = 0.07, SDL = 51.85, Kappa = 3, R^2 of trend = 0.12, NRMSE = 0.17, ME*10^{-3} = 0.68, MSDR = 0.74, R^2 of cross validation = 0.26

The entropy can be additively distributed between individual species (Table 3) or by site and thus reproduce spatial patterns of β-entropy variability induced by different factors (Figures 15–19). The species *Asperuga procumbens* L., *Galium aparine* L., and *Impatiens parviflora* DC. had a significant dependence on the PC1. The species *Anthriscus sylvestris* (L.) Hoffm., *Chelidonium majus* L., *Galium aparine* L. and *Stellaria media*

(L.) Vill had a significant dependence on the PC2. The species *Geum urbanum* L. and *Stellaria media* (L.) Vill had a significant dependence on the PC3. The species *Chelidonium majus* L., *Galium aparine* L. and *Stellaria media* (L.) Vill. were sensitive to the effect of reconstruction. The specificity of individual landfills is demonstrated by such species as *Anthriscus sylvestris* (L.) Hoffm., *Chelidonium majus* L., *Dactylis glomerata* L., *Fraxinus excelsior* L., *Impatiens parviflora* DC., *Robinia pseudoacacia* L., *Stellaria media* (L.) Vill. The species *Acer platanoides* L., *Aesculus hippocastanum* L., *Anthriscus sylvestris* (L.) Hoffm., *Chelidonium majus* L., *Galium aparine* L., *Robinia pseudoacacia* L., *Stellaria media* (L.) Vill. were sensitive to the influence of other factors that were not taken into account in this study or have a neutral nature.

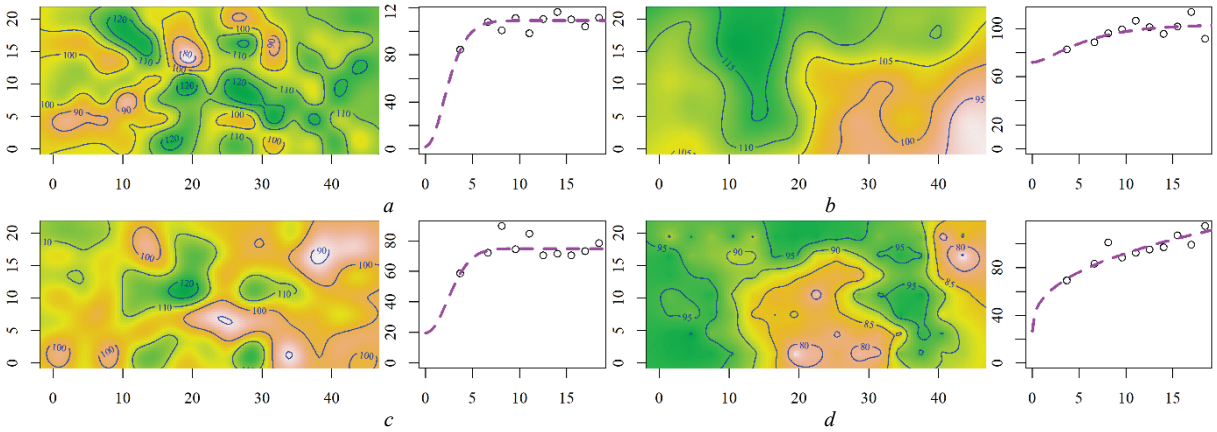

Fig. 12. The spatial variation of the phytoindication score of continentality and the variogram of the spatial model: the isoline indicates the value of the phytoindication assessment; the spatial model is shown in local coordinates; the abscissa and ordinate axes are in meters; the abscissa axis of the variogram is the distance (m); the ordinate axis is the variation; polygon a: Mean = 106.08 ± 108.66, Phi = 0.62, Practical range = 5.68, Sill = 102.74, Nugget = 6.46, SDL = 5.92, Kappa = 6.5, R^2 of trend = 0.11, NRMSE = 0.15, ME*10^{-3} = 9.55, MSDR = 1.07, R^2 of cross validation = 0.08; polygon b: Mean = 106.72 ± 100.86, Phi = 3.12, Practical range = 12.49, Sill = 39.35, Nugget = 62.89, SDL = 61.51, Kappa = 1, R^2 of trend = 0.17, NRMSE = 0.2, ME*10^{-3} = –37.26, MSDR = 0.86, R^2 of cross validation = 0.13; polygon c: Mean = 104.25 ± 76.37, Phi = 0.49, Practical range = 5.49, Sill = 70.27, Nugget = 4.56, SDL = 6.1, Kappa = 10, R^2 of trend = 0.1, NRMSE = 0.14, ME*10^{-3} = –17.54, MSDR = 0.89, R^2 of cross validation = 0.15; polygon d: Mean = 90.06 ± 126.75, Phi = 19.12, Practical range = 57.28, Sill = 87.75, Nugget = 56.11, SDL = 39, Kappa = 0.5, R^2 of trend = 0.05, NRMSE = 0.29, ME*10^{-3} = 3.91, MSDR = 0.8, R^2 of cross validation = 0.19

The factors induce changes in β-entropy which form different spatial patterns depending on the park reconstruction. Changes in β-entropy induced by the PC1 were less spatially dependent in the reconstructed sites (SDL = 49.6–51.1%) than in the unreconstructed sites (SDL = 4.6–49.6%, Fig. 15). The practical range varied considerably and could not be explained by the effect of reconstruction. The Kappa parameter indicated the homogeneity of the spatial models for describing patterns in different polygons. The spatial patterns of β-entropy changes induced by PC2 were most pronounced in the polygons that underwent reconstruction. In the polygons without reconstruction, the corresponding spatial patterns had the character of mathematical artifacts (Fig. 16). The spatial patterns of β-entropy changes induced by PC3 occurred in polygons b and d, and in the rest they had the character of mathematical artifacts (Fig. 17). Obviously, these patterns indicate the specificity of the vegetation cover, which did not depend on the park reconstruction.

The spatial patterns of β-entropy changes induced by the park reconstruction in the reconstruction zone formed strongly spatially dependent structures (SDL = 6.74–6.75%, Fig. 18). In the area without reconstruction, these structures were strongly and moderately spatially structured (SDL = 6.48–47.15%). There is a possibility that the corresponding spatial pattern in polygon c was a mathematical artifact. The practical range in the reconstruction area was 4.47–5.29 meters, and in the area without reconstruction it was 3.66–45.89 meters. The Kappa parameter indicates the heterogeneity of spatial patterns in the reconstruction zone and without reconstruction. The spatial patterns specific to the individual polygons (Fig. 19) indicate the peculiarities of the spatial structure of vegetation cover within the individual polygons.

Discussion

A key issue in ecology is understanding the role of ecosystem diversity in their functional activity and sustainability (Correia & Lopes, 2023). An ecosystem function that is viewed through the prism of human benefit is an ecosystem service (Zymaroieva et al., 2022). Vegetation cover in park plantations provides a wide range of ecosystem services (Mexia et al., 2018). The intensity of these services and the stability of their provision over time depend on the state of the vegetation, which can be characterized by its diversity. Urban parks are human-made systems that exist under conditions of intense anthropogenic impact (Pickett et al., 2011). Therefore, in order to achieve maximum values of ecosystem services and sustainability of the park system, it is necessary to apply management measures, among which reconstruction is an important tool. The study found that the reconstruction of the park significantly affects the conditions of the park's existence and the diversity of vegetation. The changes can be observed by comparing the polygons that have undergone reconstruction with those that have not. Also, the reconstruction of the park led to changes in the spatial organization of the vegetation cover.

The results indicate a decrease in soil moisture content as a result of the park's reconstruction. The conclusions based on the phytoindication approach fully coincide with the results of direct measurements of soil moisture (Kunakh et al., 2021). The decrease in soil moisture can be explained by the fact that the density of the crowns of the park's tree stand decreased after the reconstruction project. The sparse layer of canopy has become more permeable to solar energy, which contributes to higher temperatures and better ventilation. As a result, soil drying is activated. This mechanism is also confirmed by the fact an inverse correlation was found between soil moisture and forest canopy density (Zhukov et al., 2023). Obviously, reducing the density of canopies as a result of their pruning during the reconstruction process also reduces the amount of fallen leaves that form the leaf litter. The reconstruction should be noted as not being a significant factor in determining the variation of the soil moisture in the park, as it is also influenced by other factors. In turn, the reconstruction is the leading factor that determines the regime of soil moisture variability.

The phytoindication also allows us to assess the variability of regimes that are more difficult to measure than, for example, the soil moisture content. Such a regime is the regime of soil moisture variability. The results obtained indicate a significant increase in the variability of the moisture regime under the influence of the park reconstruction. The areas without reconstruction were favorable for hydrocontrastophobes (Didukh, 2011). These are plants that are adapted to moist forest and meadow habitats with uniform, stable moistening of the soil layer by groundwater and partially by surface water, where plant roots penetrate. The reconstruction

changes the conditions of plant existence in such a way that they become favorable for semi-hydro-contrastophobes. This is a group of plants that are adapted to fresh forest and meadow habitats with moderately uneven soil moisture, which is completely saturated with precipitation and meltwater. The moisture contrast scale should be emphasized as a feature of the Didukh system, which is inherited from the Ramensky scale. There is no analogy of this scale in the scales of European authors, so the patterns of changes in the moisture regime of park plantations using the phytoindication method have not been studied. However, the ecosystem service of park plantations, which consists in reducing erosion processes and redirecting lateral runoff into vertical runoff, is very important. This ecosystem service is definitely marked by the variability of moisture, since vertically redirected lateral runoff does not cause erosion and provides saturation of the soil cover with moisture, which is gradually used by the vegetation cover for vegetation. This gradualness is the antithesis of the contrasting moisture conditions. Thus, the initial effect of park reconstruction can have adverse consequences for the provision of erosion control ecosystem services provided by park plantations. Obviously, the development of a reconstruction action plan should include tools that would prevent possible negative consequences. For example, this could include planting herbaceous plants with fibrous root systems, which significantly improve the erosion control properties of the ecosystem by creating a dense sod layer.

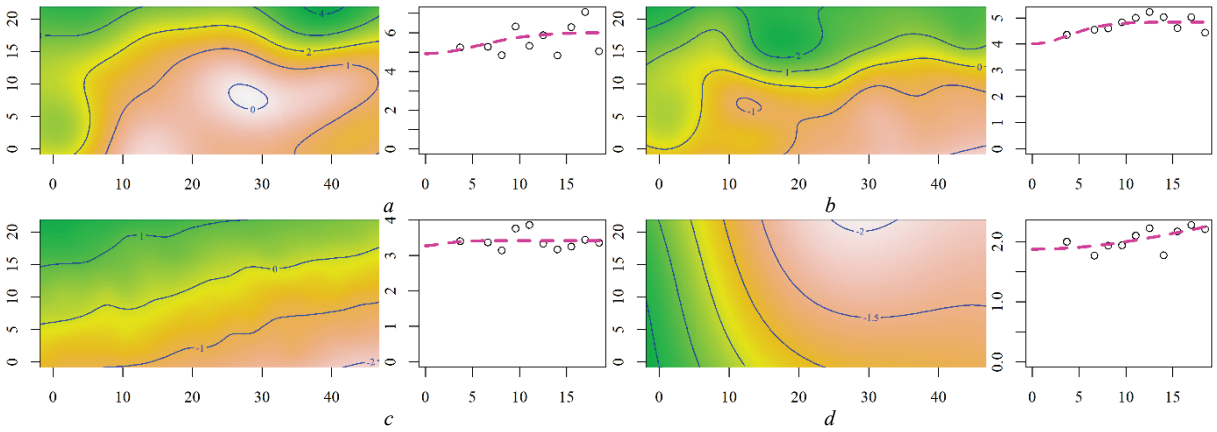

Fig. 13. The spatial variation of the cryoclimate phytoindicator score and the variogram of the spatial model: the isoline indicates the value of the phytoindication assessment; the spatial model is shown in local coordinates; the abscissa and ordinate axes are in meters; the abscissa axis of the variogram is the distance (m); the ordinate axis is the variation; polygon a: Mean = 1.64 ± 70.8, Phi = 5.5, Practical range = 16.48, Sill = 1.89, Nugget = 4.18, SDL = 68.91, Kappa = 0.5, R^2 of trend = 0.06, NRMSE = 0.31, ME*10^{-3} = 12.66, MSDR = 0.9, R^2 of cross validation = 0.09; polygon b: Mean = 0.18 ± 66.22, Phi = 1.98, Practical range = 7.91, Sill = 1.71, Nugget = 3.12, SDL = 64.51, Kappa = 1, R^2 of trend = 0.18, NRMSE = 0.22, ME*10^{-3} = 3.85, MSDR = 0.94, R^2 of cross validation = 0.05; polygon c: Mean = –0.16 ± 68.15, Phi = 0.99, Practical range = 2.97, Sill = 1.13, Nugget = 2.29, SDL = 67.02, Kappa = 0.5, R^2 of trend = 0.15, NRMSE = 0.27, ME*10^{-3} = 0.06, MSDR = 1.01, R^2 of cross validation = 0.07; Polygon d: Mean = –1.12 ± 64.26, Phi = 5.18, Practical range = 15.51, Sill = 0.8, Nugget = 1.38, SDL = 63.46, Kappa = 0.5, R^2 of trend = 0.12, NRMSE = 0.26, ME*10^{-3} = 2, MSDR = 1, R^2 of cross validation = 0.01

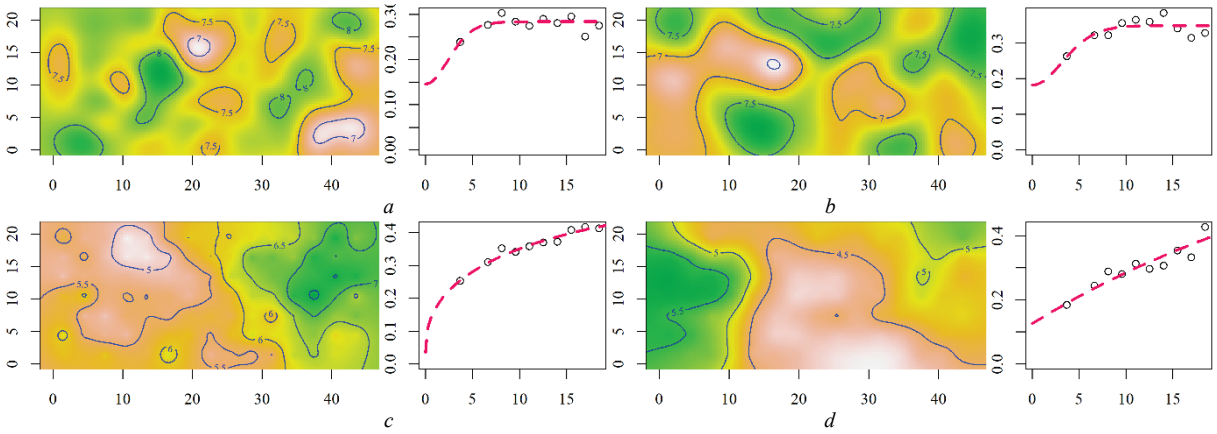

Fig. 14. The spatial variation of the phytoindication assessment of the lighting regime and the variogram of the spatial model: the isoline indicates the value of the phytoindication assessment; the spatial model is shown in local coordinates; the abscissa and ordinate axes are in meters; the abscissa axis of the variogram is the distance (m); the ordinate axis is the variation; polygon a: Mean = 7.67 ± 51.94, Phi = 0.57, Practical range = 6.37, Sill = 0.14, Nugget = 0.15, SDL = 51.8, Kappa = 10, R^2 of trend = 0.04, NRMSE = 0.25, ME*10^{-3} = –0.08, MSDR = 0.91, R^2 of cross validation = 0.09; polygon b: Mean = 7.23 ± 54.91, Phi = 0.78, Practical range = 8.74, Sill = 0.16, Nugget = 0.19, SDL = 54.75, Kappa = 10, R^2 of trend = 0.02, NRMSE = 0.27, ME*10^{-3} = 1.3, MSDR = 0.85, R^2 of cross validation = 0.14; polygon c: Mean = 5.97 ± 36.45, Phi = 12.1, Practical range = 36.24, Sill = 0.31, Nugget = 0.18, SDL = 36.14, Kappa = 0.5, R^2 of trend = 0.43, NRMSE = 0.14, ME*10^{-3} = 0.05, MSDR = 0.7, R^2 of cross validation = 0.29; polygon d: Mean = 4.77 ± 14.13, Phi = 51.84, Practical range = 155.31, Sill = 0.86, Nugget = 0.13, SDL = 13.27, Kappa = 0.5, R^2 of trend = 0.13, NRMSE = 0.17, ME*10^{-3} = 0.47, MSDR = 0.58, R^2 of cross validation = 0.42

The phytoindication suggests a decrease in the acidity of the soil solution as a result of reconstruction. The species composition of urban plantations is known to have a strong impact on soil acidity (Straigytė et al., 2019). Increased alkalinity is a typical trend in soil properties in urban parks (Jim, 1998). The stand of trees in the parks also affects the soil acidity. There is evidence that under old trees that form a stable litter, soil pH is usually consistently low. In general, older parks have lower soil pH than younger ones, but this depends on the type of vegetation (Kotze et al., 2021). Thus, the changes in the state of the forest litter in the park as a result of reconstruction may be a factor in the variation of soil acidity. The changes in soil acidity are accompanied by an increase in phytoindication estimates of carbonate content in the soil. Changes in the light regime can be assumed to create conditions favorable to species that can live in steppe environments, which are usually characterized by a higher car-

bonate content in the soil. The observed increase in carbonate content estimates may be an artifact, where representatives of another ecological group also have related ecological properties that can be misinterpreted as indicators of certain regimes. Certainly, to test this hypothesis, additional studies with instrumental measurements of soil carbonate content are needed to confirm or refute the impact of reconstruction on soil carbonate content. A similar test should be conducted for changes in soil nitrogen content. The phytoindication indicates an increase in the nitrogen content under the influence of reconstruction. However, the impact of reconstruction may favor plants belonging to the ecological group of ruderal species, which also have higher requirements for soil nutrients. That is, the mechanism of growth of phytoindication estimates of nitrogen content may be of a cenotic nature, rather than directly induced by the changes in environmental conditions. However, a real increase in soil nitrogen content as a result of reconstruction is also possible (Polevoy et al., 2023). For example, an increase in the recreational attractiveness of a park after reconstruction may increase the number of visitors with pets, which can increase the nitrogen content of the park's soil through excrement. The level of nitrogen inputs by dogs with feces and urine in park plantings significantly exceeds the level of inputs from atmospheric nitrogen inputs and the amount that can be removed through traditional nature management. Such levels of nutrient inputs can have a significant impact on biodiversity and ecosystem functioning, as well as determine the results of restoration (De Frenne et al., 2022). Even if solid waste from pets is removed from the park, the amount of nitrogen that enters the park with pet urine is very significant and depends on the number of visitors with dogs (Paradeis et al., 2013).

Table 1

The principal component analysis of variation of phytoindication assessments of environmental factors (correlation coefficients are significant for $P < 0.005$)

Variable	PC1, λ = 5.7, 47.8%	PC2, λ = 1.5, 12.8%	PC3, λ = 1.3, 10.6%
Hd	–0.24	0.83	0.16
fH	0.86	–0.12	–0.28
Rc	0.77	–0.31	0.31
Sl	–0.20	–	0.87
Ca	0.92	–	–
Nt	0.52	–0.22	–
Ae	0.77	–0.41	0.19
Tm	–0.72	–0.41	–
Om	0.83	0.30	–0.12
Kn	0.56	0.32	0.50
Cr	0.49	0.39	–0.15
Lc	0.91	–	–

The park's conditions in the absence of reconstruction are favorable for subaerophiles. The subaerophiles are plants adapted to well-aerated habitats with low to moderate moisture in the soil layer due to precipitation and meltwater. The reconstruction leads to changes in the environment and makes it more favorable for hemiaerophobes. Under natural conditions, hemiaerophobes are plants that grow on moderately aerated soils, dry clay or wet sandy soils with full moisture of the soil layer by precipitation and meltwater or temporary moisture of the soil layer by groundwater. Obviously, the reconstruction of the park results in soil compaction, which leads to a deterioration of the soil aeration regime. Visits to parks leads to soil compaction (Supuka et al., 2009). Soil compaction in urban parks promotes denitrification (Li et al., 2014), which is a consequence of the prevalence of anaerobic conditions in the soil (Davidson et al., 1986). The reduction in soil aeration is a result of soil compaction (Unger & Kaspar, 1994). In turn, plants can significantly reduce soil compaction and thus affect its aeration (Kunakh et al., 2022). Soil compaction as a result of reconstruction may be due to the use of machinery to carry out the work. Soil compaction may also be the result of more visits to the park due to improved conditions (Telyuk et al., 2022).

The phytoindication also revealed trends in the variability of microclimatic conditions in the park as a result of the reconstruction. The climatic conditions largely determine the attractiveness of urban parks (Ćwik et al., 2018). The behavioral responses, such as the dynamics of park visits, spatial and temporal patterns of distribution of park visitors, depend on air temperature and the spatial structure of vegetation in parks. The daily attendance of parks in summer decreases with the increase of the maximum daily temperature. The results of the survey show that park visitors experienced a high level of thermal comfort during all the days under study. Parks in temperate climates can guarantee a high level of thermal comfort even on the warmest days if they provide a variety of solar exposure conditions (Panchenko, 2022). The spatial typology of tree configurations for microclimatic diversity should provide a wide range of sun-exposed, semi-shaded, and shaded areas to meet the different needs of visitors. Our results suggest the reconstruction leads to the unification of the thermal regime. A significant level of variability in thermal conditions is observed in areas without reconstruction. The general trends of changes in microclimatic conditions in the park as a result of reconstruction can be explained by a decrease in the density of crown space due to crown pruning and removal of old trees. The most important observed trend is a change in the light regime, which increases the amount of solar energy reaching the soil surface. The microclimatic changes can also explain the changes in soil properties. More solar radiation and better airing lead to a higher intensity of water evaporation from the soil surface and an increase in its penetration resistance.

Table 2

The analysis of deviance, entropy, and diversity for the plant community data. PC1, PC2, and PC3 are the principal components extracted after principal component analysis of the phytoindication estimation of the ecological factors variation

Model	Degrees of freedom	Difference degrees of freedom	Deviance	Deviance difference	Entropy	Entropy difference	*P*-level	Diversity	Diversity ratio
Constant (*γ*-diversity)	17598	–	2361.4	–	2.81	–	–	16.6	–
PC1	17556	42	2082.3	279.1	2.48	0.33	<0.001	11.9	1.39
PC1 + PC2	17514	42	2013.2	69.1	2.40	0.08	0.01	11.0	1.09
PC1 + PC2 + PC3	17472	42	1982.6	30.7	2.36	0.04	0.01	10.6	1.04
PC1 + PC2 + PC3+Reconstruction	17430	42	1856.0	126.6	2.21	0.15	0.01	9.1	1.16
PC1 + PC2 + PC3+Reconstruction+Polygon	17346	84	1741.4	114.6	2.07	0.14	0.01	7.9	1.15
PC1 + PC2 + PC3+Reconstruction+ Polygon + Site (*α*-diversity)	0	17346	1322.9	418.4	1.57	0.50	–	4.8	1.65

The park reconstruction leads not only to changes in the modal levels of ecological regimes, but also to the formation of specific patterns of their spatial distribution. The phytoindication variables form spatially organized patterns, which suggests their non-random variability within the polygons. The reasons for the spatial heterogeneity of vegetation cover at the mesolevel may be the terrain features (Frouz et al., 2011), heterogeneity of soil properties (Lesschen et al., 2008), interaction between plants (Bloor et al., 2020), animal influence (Adler et al., 2001), as well as the effect of neutral factors (Maaß et al., 2015). The recreational load and anthropogenic impact in urban parks can generate spatial patterns of vegetation cover (Fornal-Pieniak et al., 2019). The spatial structure of the vegetation cover is in the form of patches with a non-randomly similar composition of plant species, which differ to some extent from other patches. Such areas have a certain configuration and most typical dimensions. The phytoindication scales demonstrate spatial patterns as a result of the coordinated dynamics of ecologically similar plant species in a gradient of certain environmental factors. Thus, phytoindication scales allow us to identify the level of homogeneity or heterogeneity of vegetation cover and to understand the causes of spatial patterns as a response to environmental factors.

The practical range is a measure of the typical size of homogeneous plots in terms of geostatistical analysis. The practical range of variograms describing the spatial behavior of phytoindication scales decreases under the influence of reconstruction. This indicates heterogenization of the ecological space under the influence of reconstruction. Heterogenization is

manifested in the fact that patches of vegetation with homogeneous vegetation cover in terms of environmental conditions are decreasing. The environmental variations in a natural landscape are often continuous, variations exist within patches, and patches rarely have clearly defined boundaries. Heterogeneity can be described by analogy to a physical surface. A homogeneous surface is smooth, and similar values are aggregated. As the aggregation of similar values decreases, the surface becomes increasingly rough. The concept of "roughness" has been proposed as a new term to describe the spatial configuration for continuous variables and as a continuous equivalent of a discrete measure of aggregation of sites (Dufour et al., 2006). The fractal dimension can be used to estimate the topographic roughness (Palmer, 1992). The fractal dimension of a spatial process can be estimated from the variogram parameters (Gneiting et al., 2012).

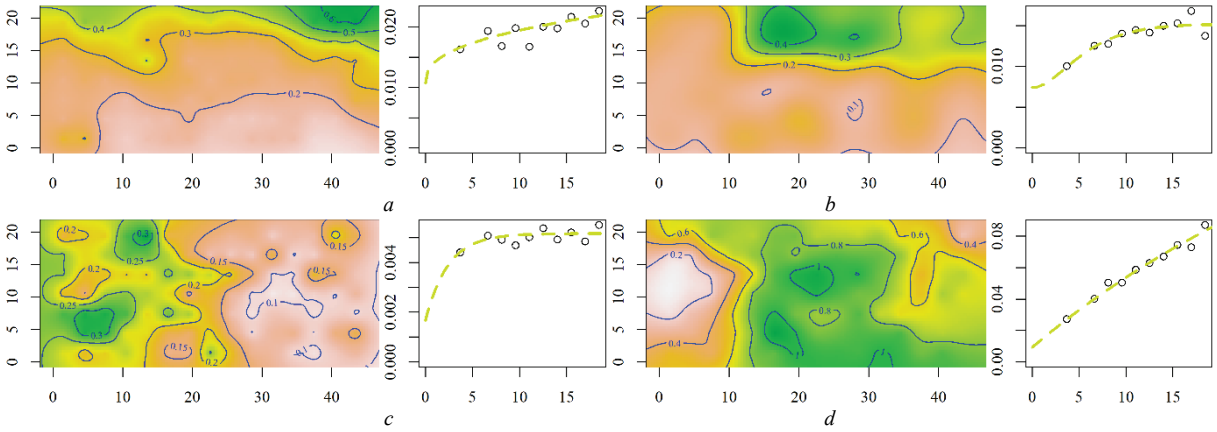

Fig. 15. The spatial variation of the differential entropy of the plant community induced by the PC1 and the variogram of the spatial model: the isoline indicates the value of differential entropy; the spatial model is shown in local coordinates; the abscissa and ordinate axes are given in meters; the abscissa axis of the variogram is the distance (m); the ordinate axis is the variation; polygon a: Mean = 0.28 ± 0.03, Phi = 30.25, Practical range = 90.64, Sill = 0.015, Nugget = 0.015, SDL = 49.6, Kappa = 0.5, R^2 of trend = 0.22, NRMSE = 0.22, ME*10^{-3} = 0, MSDR = 0.91, R^2 of cross validation = 0.09; polygon b: Mean = 0.19 ± 0.015, Phi = 2.34, Practical range = 13.84, Sill = 0.007, Nugget = 0.008, SDL = 51.06, Kappa = 2.5, R^2 of trend = 0.25, NRMSE = 0.14, MSDR = 0.71, R^2 of cross validation = 0.29; polygon c: Mean = 0.18 ± 0.01, Phi = 2.4, Practical range = 7.19, Sill = 0.003, Nugget = 0.002, SDL = 32.51, Kappa = 0.5, R^2 of trend = 0.3, NRMSE = 0.16, ME*10^{-3} = 0, MSDR = 0.89, R^2 of cross validation = 0.1; polygon d: Mean = 0.68 ± 0.19, Phi = 35.21, Practical range = 105.47, Sill = 0.18, Nugget = 0.009, SDL = 4.57, Kappa = 0.5, R^2 of trend = 0.16, NRMSE = 0.1, ME*10^{-3} = 0, MSDR = 0.4, R^2 of cross validation = 0.59

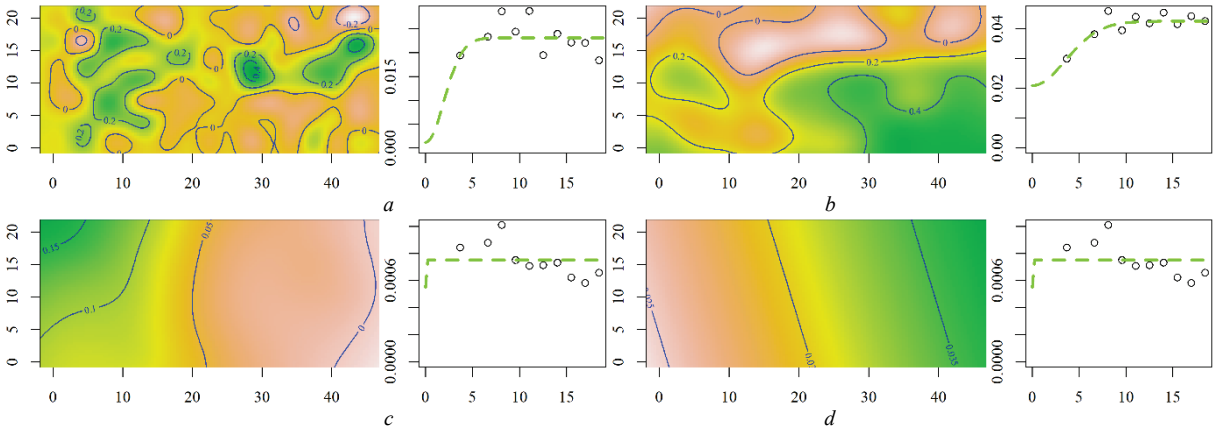

Fig. 16. The spatial variation of the differential entropy of the plant community induced by PC2 and the variogram of the spatial model: the isoline indicates the value of differential entropy; the spatial model is shown in local coordinates; the abscissa and ordinate axes are given in meters; the abscissa axis of the variogram is the distance (m); the ordinate axis is the variation; polygon a: Mean = 0.05 ± 0.02, Phi = 0.44, Practical range = 4.92, Sill = 0.022, Nugget = 0.002, SDL = 6.71, Kappa = 10, R^2 of trend = 0.04, NRMSE = 0.15, ME*10^{-3} = –1.09, MSDR = 0.88, R^2 of cross validation = 0.13; polygon b: Mean = 0.19 ± 0.04, Phi = 1.11, Practical range = 8.98, Sill = 0.024, Nugget = 0.019, SDL = 43.76, Kappa = 5, R^2 of trend = 0.33, NRMSE = 0.12, ME*10^{-3} = 0.72, MSDR = 0.62, R^2 of cross validation = 0.38; polygon c: Mean = 0.05 ± 0.008, Phi = 9.8, Practical range = 29.35, Sill = 0.003, Nugget = 0.005, SDL = 62.44, Kappa = 0.5, R^2 of trend = 0.18, NRMSE = 0.29, R2 of cross validation = 0.01; polygon d: Mean = 0.03 ± 0.001, Phi = 0.08, Practical range = 0.84, Sill = 0.001, SDL = 14.57, Kappa = 9.5, R^2 of trend = 0.01, NRMSE = 0.15, ME*10^{-3} = 0, MSDR = 1.01, R^2 of cross validation = 1

The accuracy of the description of the spatial process was found to decrease after the park reconstruction procedures. Obviously, the park reconstruction disrupts the course of long-term processes that provide structuring of the vegetation cover, resulting in the temporal and spatial dissynchronization of the dynamics of ecological processes (Kunakh et al., 2022). The spatial variation of variables that indicate soil processes can best be described. By contrast, the phytoindication scales that indicate climatic factors are much less spatially structured. Under the influence of reconstruction, the best variogram model for describing a spatial process also changes. The Gaussian model is most often the most adequate for conditions without reconstruction, and the exponential model is most often the best model for conditions after reconstruction. In other words, these transformations can be described as a transition from a "smoothed" to a "rough" spatial process under the influence of park reconstruction. The smoothness and roughness of the spatial process that can be used to describe the soil surface is of functional importance for assessing erosion risks. Under the conditions of a fixed variogram model, the ratio of the nugget effect and the partial threshold is used to describe the smoothness and roughness (Jan Vermang et al., 2013). The diversity of plant communities is influenced by two aspects of spatial heterogeneity. These are the variability of environmental conditions, which determines the number of habitat types, and the spatial configuration of habitats, which affects the

speed of ecological processes such as dispersal or competition. Species richness generally increases with increasing environmental variability and "roughness", i.e. with decreasing spatial aggregation (Dufour et al., 2006). A similar effect was found in our study. The increase in the "roughness" of spatial variability of vegetation cover under the influence of reconstruction was accompanied by an increase in species diversity of the community.

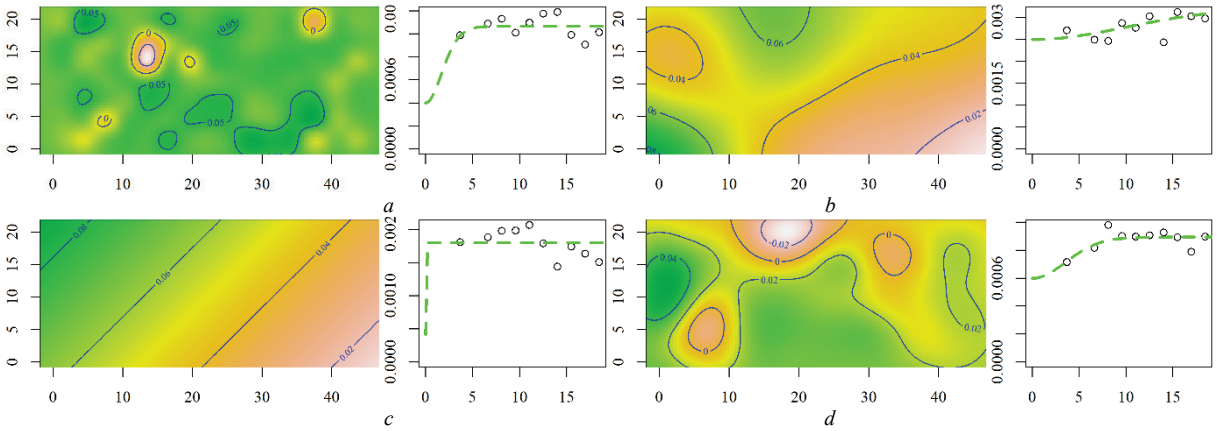

Fig. 17. The spatial variation of the differential entropy of the plant community induced by PC3 and the variogram of the spatial model: the isoline indicates the value of differential entropy; the spatial model is shown in local coordinates; the abscissa and ordinate axes are given in meters; the abscissa axis of the variogram is the distance (m); the ordinate axis is the variation; polygon a: Mean = 0.04 ± 0.001, Phi = 0.4, Practical range = 4.48, Sill = 0.001, Nugget = 0, SDL = 39.23, Kappa = 10, R^2 of trend = 0.01, NRMSE = 0.2, ME*10^{-3} = –0.01, MSDR = 1, R^2 of cross validation = 0.01; polygon b: Mean = 0.04 ± 0.003, Phi = 14.44, Practical range = 43.25, Sill = 0.001, Nugget = 0.002, SDL = 63.88, Kappa = 0.5, R^2 of trend = 0.02, NRMSE = 0.43, ME*10^{-3} = 0.11, MSDR = 1.07, R^2 of cross validation = 0.02; polygon c: Mean = 0.05 ± 0.002, Phi = 0.2, Practical range = 0.6, Sill = 0.001, Nugget = 0.001, SDL = 38.23, Kappa = 0.5, R^2 of trend = 0.12, NRMSE = 0.25, ME*10^{-3} = 0, MSDR = 1.01, R^2 of cross validation = 1; polygon d: Mean = 0.02 ± 0.001, Phi = 0.8, Practical range = 8.53, Sill = 0, Nugget = 0.001, SDL = 60, Kappa = 9, R^2 of trend = 0.04, NRMSE = 0.23, ME*10^{-3} = 0.02, MSDR = 0.8, R^2 of cross validation = 0.19

The ecological scales are formally nominally independent, but in reality, at a certain spatial level, they demonstrate the coordinated dynamics of a complex of environmental factors. The principal component 1, which was extracted after the analysis of the principal components of variability of the phytoindication scales, represents the result of variability of environmental conditions driven by changes in the light regime in the park as a result of reconstruction. The change in light regime is a moderator of changes in the variability of moisture, acidity, carbonate content, nitrogen content, soil aeration, ombroclimate, continentality, and cryoclimate. Our results are in line with the data according to which the temperature gradients of urban parks are influenced by both the horizontal movement of cold or warm air masses over the parks and evaporation from trees, which creates an island of coolness (Chang & Li, 2014). The reconstruction of the park significantly changes the light regime, which affects a set of processes that covers both the climatic and soil components of the park plantation. The change in the light regime cannot be interpreted unambiguously. In the summer, such changes can be seen as somewhat worsening the conditions for visitors to the park and worsening ecological regimes. Increased insolation can lead to a deterioration of the thermal regime in the park, and can stimulate excessive drying of the soil and deterioration of its physical properties. On the other hand, in the spring, early warming of the soil surface improves the conditions for visitors during this period of the year and promotes the formation of a greater diversity of plants (Zhukov et al., 2017), including early spring ephemerals, among which rare species are often found. Higher insolation in spring extends the period of active life of soil animals, when the time of sufficient soil moisture content coincides with optimal temperature conditions. The longer activity of soil animals can accelerate the restoration of the physical condition of the soil and speed up the processes of the nutrient cycle (Tutova et al., 2022).

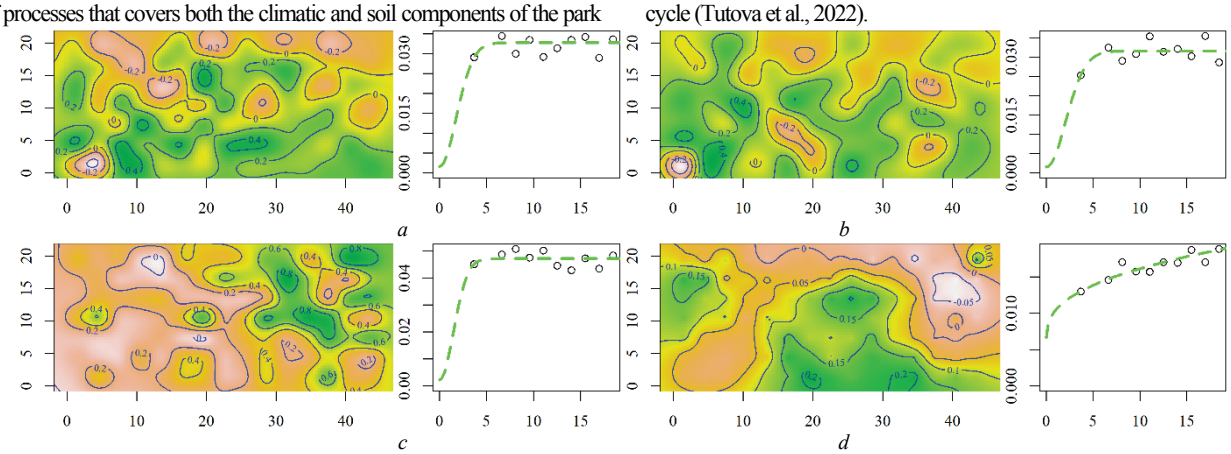

Fig. 18. The spatial variation of the differential entropy of the plant community induced by the reconstruction and the variogram of the spatial model: the isoline indicates the value of differential entropy; the spatial model is shown in local coordinates; the abscissa and ordinate axes are given in meters; the abscissa axis of the variogram is the distance (m); the ordinate axis is the variation; polygon a: Mean = 0.05 ± 0.007, Phi = 0.6, Practical range = 5.49, Sill = 0.006, Nugget = 0, SDL = 6.58, Kappa = 6.5, R^2 of trend = 0.1, NRMSE = 0.15, ME*10^{-3} = 0.86, MSDR = 0.86, R^2 of cross validation = 0.17; polygon b: Mean = 0.11 ± 0.002, Phi = 2.4, Practical range = 7.19, Sill = 0.001, Nugget = 0.001, SDL = 66.67, Kappa = 0.5, R^2 of trend = 0.16, NRMSE = 0.2, ME*10^{-3} = 0.05, MSDR = 0.97, R^2 of cross validation = 0.02; polygon c: Mean = 0.26 ± 0.078, Phi = 0.96, Practical range = 6.19, Sill = 0.029, Nugget = 0.049, SDL = 63.02, Kappa = 3, R^2 of trend = 0.19, NRMSE = 0.2, ME*10^{-3} = –0.15, MSDR = 0.96, R^2 of cross validation = 0.03; polygon d: Mean = 0.14 ± 0.045, Phi = 16.6, Practical range = 49.72, Sill = 0.038, Nugget = 0.007, SDL = 14.61, Kappa = 0.5, R^2 of trend = 0.06, NRMSE = 0.18, ME*10^{-3} = –0.31, MSDR = 0.58, R^2 of cross validation = 0.41

Soil moisture variation was a factor statistically independent of light regime variability. The soil moisture regime also varies in conjunction with other phytoindication scales such as ombroclimate, continentality, cryoclimate, moisture variability, soil acidity, nitrogen content, aeration, and thermal climate. Another important aspect of the variability of environmental conditions within the park is the aeration regime. Both the humidity regime and the aeration regime indicate the peculiarities of environmental conditions within the park, which exist regardless of the influence of the reconstruction factor. The eigenvalues of the principal components allow us to compare their contribution to explaining the variability of environmental indicators. The principal component 1, which depends on the park's reconstruction, explains 47.8% of the variation in phytoindication scales, and the principal components 2 and 3, which do not depend on the park's reconstruction, explain 23.4% together. Thus, the impact of the park reconstruction on the vegetation cover is very significant and it outweighs the impact of natural variability of environmental conditions in the park by almost two times.

The impact of the park reconstruction leads to the formation of beta-diversity of the plant community, which may include patterns caused by the transformation of environmental conditions and can be determined using phytoindication scales. The impact of the park reconstruction on the beta diversity of the plant community consists of the impact of principal component 1 and other changes, which are comprehensively denoted by the nominal variable "Impact of reconstruction". The principal component 1 is able to explain 26.6% of the beta diversity, while other reasons related to the park reconstruction were able to explain 12.1% of the beta diversity. Thus, the reconstruction can significantly change the conditions of plants' existence, and the plant community can change its organization accordingly so that the variation in beta diversity is consistent and can be reflected in changes in phytoindication scales.

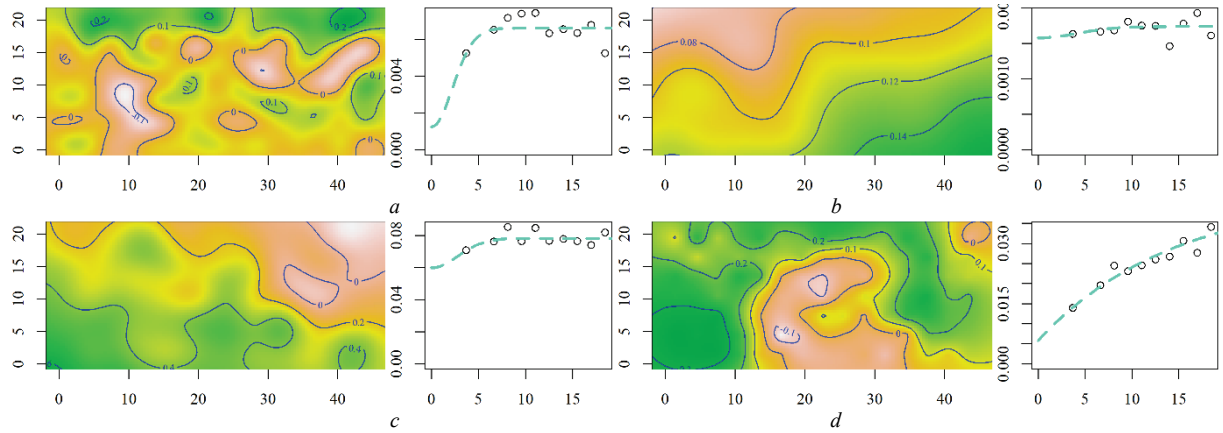

Fig. 19. The spatial variation of the differential entropy of the plant community induced by the influence of features within the polygons and the variogram of the spatial model: the isoline indicates the value of differential entropy; the spatial model is shown in local coordinates; the abscissa and ordinate axes are given in meters; the abscissa axis of the variogram is the distance (m); the ordinate axis is the variation; polygon a: Mean = 0.08 ± 0.03, Phi = 0.4, Practical range = 4.47, Sill = 0.031, Nugget = 0.002, SDL = 6.74, Kappa = 10, R^2 of trend = 0.21, NRMSE = 0.12, ME*10^{-3} = –0.75, MSDR = 0.94, R^2 of cross validation = 0.07; polygon b: Mean = 0.10 ± 0.03, Phi = 0.47, Practical range = 5.29, Sill = 0.029, Nugget = 0.002, SDL = 6.75, Kappa = 10, R^2 of trend = 0.1, NRMSE = 0.12, ME*10^{-3} = –0.72, MSDR = 0.93, R^2 of cross validation = 0.1; polygon c: Mean = 0.34 ± 0.05, Phi = 0.33, Practical range = 3.66, Sill = 0.044, Nugget = 0.003, SDL = 6.48, Kappa = 10, R^2 of trend = 0.32, NRMSE = 0.13, ME*10^{-3} = 0.1, MSDR = 0.9, R^2 of cross validation = 0.12; Polygon d: Mean = 0.07 ± 0.02, Phi = 15.32, Practical range = 45.89, Sill = 0.012, Nugget = 0.01, SDL = 47.15, Kappa = 0.5, R^2 of trend = 0.06, NRMSE = 0.29, ME*10^{-3} = 0.37, MSDR = 0.89, R^2 of cross validation = 0.1

Table 3

The contribution of each plant species to the Shannon entropy of the community and to the entropy of the community fractionated according to the influence of the principal components of variation in phytoindicator estimates of environmental factors (the entropy values that decrease the most under the influence of the respective predictor are marked*)

Species	Constant (γ-diversity)	PC1	PC2	PC3	Reconstruction	Polygon	Sites (α-diversity)
Acer negundo L.	0.043	0.035	0.034	0.034	0.033	0.030	0.028
A. platanoides L.	0.239	0.213	0.212	0.211	0.213	0.197	0.153*
Aesculus hippocastanum L.	0.087	0.081	0.079	0.078	0.079	0.078	0.048*
Alliaria petiolata (M.Bieb.) Cavara et Grande	0.062	0.061	0.059	0.057	0.058	0.056	0.043
Anthriscus sylvestris (L.) Hoffm.	0.210	0.203	0.196*	0.195	0.118	0.097*	0.072*
Arctium minus (Hill) Bernh.	0.069	0.060	0.058	0.057	0.057	0.053	0.042
Asperugo procumbens L.	0.125	0.089*	0.088	0.085	0.084	0.084	0.068
Ballota nigra L.	0.015	0.015	0.015	0.013	0.013	0.012	0.009
Bromus tectorum L.	0.015	0.014	0.014	0.014	0.014	0.014	0.009
Capsella bursa-pastoris (L.) Medik.	0.010	0.009	0.009	0.009	0.009	0.008	0.007
Carex spicata Huds.	0.027	0.026	0.026	0.026	0.026	0.026	0.019
Chaerophyllum temulum L.	0.008	0.008	0.008	0.008	0.008	0.008	0.006
Chelidonium majus L.	0.178	0.161	0.141*	0.141	0.135*	0.127*	0.100*
Chenopodium album L.	0.005	0.005	0.004	0.004	0.004	0.004	0.003
Cirsium arvense (L.) Scop.	0.006	0.005	0.005	0.005	0.005	0.005	0.004
Corydalis solida (L.) Clairv.	0.011	0.010	0.010	0.010	0.010	0.009	0.006
Dactylis glomerata L.	0.050	0.044	0.041	0.040	0.038	0.032*	0.024
Fraxinus excelsior L.	0.059	0.055	0.054	0.054	0.054	0.043*	0.029
Fumaria schleicheri Soy.-Will.	0.001	0.001	0.001	0.001	0.001	0.001	0.001
Galium aparine L.	0.307	0.245*	0.236*	0.235	0.203*	0.203	0.168*
Geum urbanum L.	0.152	0.147	0.145	0.136*	0.135	0.131	0.106
Gleditsia triacanthos L.	0.034	0.033	0.032	0.032	0.030	0.030	0.014
Hordeum murinum subsp. *leporinum* (Link) Arcang.	0.004	0.004	0.004	0.003	0.003	0.003	0.002

Species	Constant (γ-diversity)	PC1	PC2	PC3	Reconstruction	Polygon	Sites (α-diversity)
Humulus lupulus L.	0.010	0.010	0.009	0.009	0.009	0.009	0.007
Impatiens parviflora DC.	0.240	0.147*	0.147	0.147	0.144	0.135*	0.109
Jacobaea vulgaris Gaertn.	0.002	0.002	0.002	0.002	0.002	0.002	0.001
Lactuca tatarica (L.) C.A.Mey	0.010	0.010	0.010	0.010	0.009	0.008	0.007
Lapsana communis L.	0.014	0.012	0.012	0.011	0.011	0.010	0.007
Myosotis laxa subsp. *caespitosa* (Schultz) Hyl. ex Nordh.	0.031	0.030	0.029	0.029	0.027	0.027	0.022
Oxalis dillenii Jacq.	0.005	0.004	0.004	0.004	0.004	0.003	0.002
Parthenocissus quinquefolia (L.) Planch.	0.002	0.002	0.002	0.002	0.002	0.002	0.001
Poa angustifolia L.	0.007	0.007	0.007	0.007	0.007	0.007	0.004
P. annua L.	0.003	0.002	0.002	0.002	0.002	0.002	0.001
P. nemoralis L.	0.031	0.031	0.030	0.029	0.026	0.026	0.020
Quercus robur L.	0.047	0.044	0.043	0.040	0.036	0.031	0.012
Robinia pseudoacacia L.	0.151	0.145	0.146	0.145	0.144	0.138*	0.089*
Solidago canadensis L.	0.024	0.022	0.022	0.021	0.020	0.017	0.014
Stellaria media (L.) Vill	0.231	0.221	0.196*	0.191*	0.183*	0.161*	0.126*
Taraxacum campylodes G.E.Haglund	0.080	0.073	0.073	0.073	0.072	0.072	0.063
Tilia platyphyllos subsp. *cordifolia* (Besser) C.K.Schneid.	0.046	0.042	0.042	0.042	0.042	0.039	0.015
Urtica dioica L.	0.022	0.021	0.021	0.021	0.018	0.017	0.015
Veronica arguteserrata Regel & Schmalh	0.043	0.035	0.035	0.034	0.034	0.030	0.026
Viola odorata L.	0.096	0.093	0.093	0.091	0.089	0.087	0.075
Total diversity	2.811	2.479	2.397	2.360	2.210	2.073	1.575

These scales allow a meaningful interpretation of the nature of changes in the ecological environment caused by the park's reconstruction. It should be noted that in conditions without reconstruction, the organizing role of environmental factors for the variation of beta-diversity is much smaller. The contribution of principal components 2 and 3 is 9.7% to the formation of beta diversity. Whereas other factors of beta diversity that are not related to reconstruction have a contribution of 11.3% (interpolygon features) and 40.3% (alpha diversity). Inter-polygon features and alpha diversity do not correlate with phytoindication scales and are white noise in relation to the scales. This indicates that the role of phytoindication scales as an information signal for characterizing environmental conditions is buried in noise both at the interplot and intraplot levels. The reason for this phenomenon may be that park plantations without reconstruction are in the phase of naturalization and stabilization of ecological processes, and the plant species that make up them are in optimal conditions and therefore are poor indicators of environmental conditions. The reconstruction significantly and rapidly changes the environmental conditions to which not all species are well adapted, so a plant community consisting of species that exist under conditions that are far from optimal is a good indicator of environmental conditions.

In terms of further research, it is of particular interest to identify patterns of temporal dynamics of ecological regimes established using phytoindication scales. The connection between the characteristics of the species diversity of plant communities in park plantations and the ecosystem services they provide is also important. A connection between the spatial organization of plant communities and ecosystem services of park plantations can be assumed. It is also worth testing the hypothesis that the optimal conditions for the existence of plant species before the park's reconstruction are replaced by pessimistic conditions after the reconstruction.

Conclusion

The phytoindication scales are a reliable source of information for assessing the state of the vegetation cover of park plantations. The phytoindication approach allows us to identify changes in ecological regimes that occur as a result of park reconstruction and to separate them from ecological regimes of natural origin. The reconstruction of the park leads to a significant change in the light regime of the park plantations, which leads to changes in the vegetation cover and soil of the park. The variability in time and spatial heterogeneity of ecological processes are significant consequences of the park reconstruction. Smooth spatial structures of the park's vegetation cover without reconstruction are changing to rough spatial structures of the park after reconstruction. The ratio of useful phytoindication information compared to information noise in the structure of beta-diversity of the park plantation increases significantly as a result of the park reconstruction, probably due to the fact that many plant species are shifted from the optimum to the pessimistic zone.

References

Ahrné, K., Bengtsson, J., & Elmqvist, T. (2009). Bumble bees (*Bombus* spp.) along a gradient of sncreasing urbanization. PLoS One, 4(5), e5574.

Al-Shammary, A. A. G., Kouzani, A. Z., Kaynak, A., Khoo, S. Y., Norton, M., & Gates, W. (2018). Soil bulk density estimation methods: A review. Pedosphere, 28(4), 581–596.

Aydin, M., Yano, T., Evrendilek, F., & Uygur, V. (2008). Implications of climate change for evaporation from bare soils in a Mediterranean environment. Environmental Monitoring and Assessment, 140(1–3), 123–130.

Bae, J., & Ryu, Y. (2015). Land use and land cover changes explain spatial and temporal variations of the soil organic carbon stocks in a constructed urban park. Landscape and Urban Planning, 136, 57–67.

Balázs, D., Bernadett, H., & Tóthmérész, B. (2016). Grassland vegetation in urban habitats – Testing ecological theories. Tuexenia, 36, 379–393.

Barik, K., Aksakal, E. L., Islam, K. R., Sari, S., & Angin, I. (2014). Spatial variability in soil compaction properties associated with field traffic operations. Catena, 120, 122–133.

Błaszczyk, M., Suchocka, M., Wojnowska-Heciak, M., & Muszyńska, M. (2020). Quality of urban parks in the perception of city residents with mobility difficulties. PeerJ, 8, e10570.

Bodnaruk, E. W., Kroll, C. N., Yang, Y., Hirabayashi, S., Nowak, D. J., & Endreny, T. A. (2017). Where to plant urban trees? A spatially explicit methodology to explore ecosystem service tradeoffs. Landscape and Urban Planning, 157, 457–467.

Boldrin, D., Knappett, J. A., Leung, A. K., Brown, J. L., Loades, K. W., & Bengough, A. G. (2022). Modifying soil properties with herbaceous plants for natural flood risk-reduction. Ecological Engineering, 180, 106668.

Bolund, P., & Hunhammar, S. (1999). Ecosystem services in urban areas. Ecological Economics, 29(2), 293–301.

Chan, C.-S., Marafa, L. M., & Van Den Bosch, C. C. K. (2014). Changing perspectives in urban park management: A longitudinal study of Hong Kong. Managing Leisure, 20(1), 56–76.

Chan, C.-S., Si, F. H., & Marafa, L. M. (2018). Indicator development for sustainable urban park management in Hong Kong. Urban Forestry and Urban Greening, 31, 1–14.

Chiesura, A. (2004). The role of urban parks for the sustainable city. Landscape and Urban Planning, 68(1), 129–138.

Connell, J. H. (1978). Diversity in tropical rain forests and coral reefs. Science, 199(4335), 1302–1310.

Davies, R., & Hall, S. J. (2010). Direct and indirect effects of urbanization on soil and plant nutrients in desert ecosystems of the Phoenix metropolitan area, Arizona (USA). Urban Ecosystems, 13(3), 295–317.

Derkzen, M. L., van Teeffelen, A. J. A., & Verburg, P. H. (2015). Quantifying urban ecosystem services based on high-resolution data of urban green space: An assessment for Rotterdam, the Netherlands. Journal of Applied Ecology, 52(4), 1020–1032.

Faly, L. I., & Brygadyrenko, V. V. (2014). Patterns in the horizontal structure of litter invertebrate communities in windbreak plantations in the steppe zone of the Ukraine. Journal of Plant Protection Research, 54(4), 414–420.

Fehrenbach, H., Grahl, B., Giegrich, J., & Busch, M. (2015). Hemeroby as an impact category indicator for the integration of land use into life cycle (impact) assessment. International Journal of Life Cycle Assessment, 20(11), 1511–1527.

Frank, D., & Klotz, S. (1990). Biologisch-Ökologische Daten zur Flora der DDR. Wissenschaftliche Beiträge der Martin-Luther-Universität Halle-Wittenberg, Martin-Luther-Universität.
Gómez-Baggethun, E., & Barton, D. N. (2013). Classifying and valuing ecosystem services for urban planning. Ecological Economics, 86, 235–245.
Goncharenko, I., & Kovalenko, O. (2019). Oak forests of the class *Quercetea pubescentis* in Central-Eastern Ukraine. Thaiszia, 29(2), 191–215.
Goncharenko, I., Semenishchenkov, Y., Tsakalos, J. L., & Mucina, L. (2020). Thermophilous oak forests of the steppe and forest-steppe zones of Ukraine and Western Russia. Biologia, 75(3), 337–353.
Gratani, L., Varone, L., & Bonito, A. (2016). Carbon sequestration of four urban parks in Rome. Urban Forestry and Urban Greening, 19, 184–193.
Haase, D., Larondelle, N., Andersson, E., Artmann, M., Borgström, S., Breuste, J., Gomez-Baggethun, E., Gren, Å., Hamstead, Z., Hansen, R., Kabisch, N., Kremer, P., Langemeyer, J., Rall, E. L., McPhearson, T., Pauleit, S., Qureshi, S., Schwarz, N., Voigt, A., … Elmqvist, T. (2014). A quantitative review of urban ecosystem service assessments: Concepts, models, and implementation. Ambio, 43(4), 413–433.
Hajzeri, A. (2021). The management of urban parks and its contribution to social interactions. Arboricultural Journal, 43(3), 187–195.
Halecki, W., Stachura, T., Fudała, W., Stec, A., & Kuboń, S. (2023). Assessment and planning of green spaces in urban parks: A review. Sustainable Cities and Society, 88, 104280.
Heger, T. (2016). Light availability experienced in the field affects ability of following generations to respond to shading in an annual grassland plant. Journal of Ecology, 104(5), 1432–1440.
Hermy, M., & Cornelis, J. (2000). Towards a monitoring method and a number of multifaceted and hierarchical biodiversity indicators for urban and suburban parks. Landscape and Urban Planning, 49(3–4), 149–162.
Jo, H.-K., & McPherson, G. E. (1995). Carbon storage and flux in urban residential greenspace. Journal of Environmental Management, 45(2), 109–133.
Knapp, A. K., Beier, C., Briske, D. D., Classen, A. T., Luo, Y., Reichstein, M., Smith, M. D., Smith, S. D., Bell, J. E., Fay, P. A., Heisler, J. L., Leavitt, S. W., Sherry, R., Smith, B., & Weng, E. (2008). Consequences of more extreme precipitation regimes for terrestrial ecosystems. BioScience, 58(9), 811–821.
Kroetsch, D., & Wang, C. (2008). Particle size distibution. In: Carter, M. R., & Gregorich, E. G. (Eds.). Soil sampling and methods of analysis. CRC Press. Pp. 713–726.
Kühn, I., & Klotz, S. (2006). Urbanization and homogenization – Comparing the floras of urban and rural areas in Germany. Biological Conservation, 127(3), 292–300.
Kunakh, O. M., Lisovets, O. I., Yorkina, N. V., & Zhukova, Y. O. (2021). Phytoindication assessment of the effect of reconstruction on the light regime of an urban park. Biosystems Diversity, 29(3), 84–93.
Kunakh, O. M., Yorkina, N. V., Turovtseva, N. M., Bredikhina, J. L., Balyuk, J. O., & Golovnya, A. V. (2021). Effect of urban park reconstruction on physical soil properties. Ecologia Balkanica, 13(2), 57–73.
Kunakh, O. M., Yorkina, N. V., Zhukov, O. V., Turovtseva, N. M., Bredikhina, Y. L., & Logvina-Byk, T. A. (2020). Recreation and terrain effect on the spatial variation of the apparent soil electrical conductivity in an urban park. Biosystems Diversity, 28(1), 3–8.
Kunakh, O. M., Zhukov, O. V., Zots, F. A., & Molozhon, K. O. (2022). The impact of urban park reconstruction on the aggregate structure of soil. Agrology, 1(5), 15–26.
LaPaix, R., & Freedman, B. (2010). Vegetation structure and composition within urban parks of Halifax regional municipality, Nova Scotia, Canada. Landscape and Urban Planning, 98(2), 124–135.
Leff, J. W., Jones, S. E., Prober, S. M., Barberán, A., Borer, E. T., Firn, J. L., Harpole, W. S., Hobbie, S. E., Hofmockel, K. S., Knops, J. M. H., McCulley, R. L., La Pierre, K., Risch, A. C., Seabloom, E. W., Schütz, M., Steenbock, C., Stevens, C. J., & Fierer, N. (2015). Consistent responses of soil microbial communities to elevated nutrient inputs in grasslands across the globe. Proceedings of the National Academy of Sciences, 112(35), 10967–10972.
Löf, M., Madsen, P., Metslaid, M., Witzell, J., & Jacobs, D. F. (2019). Restoring forests: Regeneration and ecosystem function for the future. New Forests, 50(2), 139–151.
López-Vicente, M., Poesen, J., Navas, A., & Gaspar, L. (2013). Predicting runoff and sediment connectivity and soil erosion by water for different land use scenarios in the Spanish Pre-Pyrenees. Catena, 102, 62–73.
Mayer, H. (1999). Air pollution in cities. Atmospheric Environment, 33(24–25), 4029–4037.
McKinney, M. L. (2006). Urbanization as a major cause of biotic homogenization. Biological Conservation, 127(3), 247–260.
Mexia, T., Vieira, J., Príncipe, A., Anjos, A., Silva, P., Lopes, N., Freitas, C., Santos-Reis, M., Correia, O., Branquinho, C., & Pinho, P. (2018). Ecosystem services: Urban parks under a magnifying glass. Environmental Research, 160, 469–478.
Mileusnić, Z. I., Saljnikov, E., Radojević, R. L., & Petrović, D. V. (2022). Soil compaction due to agricultural machinery impact. Journal of Terramechanics, 100, 51–60.
Moreno, F., Pelegrín, F., Fernández, J. E., & Murillo, J. M. (1997). Soil physical properties, water depletion and crop development under traditional and conservation tillage in Southern Spain. Soil and Tillage Research, 41(1–2), 25–42.
Nidzgorski, D. A., & Hobbie, S. E. (2016). Urban trees reduce nutrient leaching to groundwater. Ecological Applications, 26(5), 1566–1580.
Niemelä, J. (1999). Ecology and urban planning. Biodiversity and Conservation, 8, 119–131.
Pauleit, S., Slinn, P., Handley, J., & Lindley, S. (2003). Promoting the natural greenstructure of towns and cities: English nature's accessible natural greenspace standards model. Built Environment, 29(2), 157–170.
Putchkov, A. V., Brygadyrenko, V. V., & Markina, T. Y. (2019). Ground beetles of the tribe Carabini (Coleoptra, Carabidae) in the main megapolises of Ukraine. Vestnik Zoologii, 53(1), 3–12.
Sarah, P., Zhevelev, H. M., & Oz, A. (2015). Urban park soil and vegetation: Effects of natural and anthropogenic factors. Pedosphere, 25(3), 392–404.
Setälä, H., Francini, G., Allen, J. A., Jumpponen, A., Hui, N., & Kotze, D. J. (2017). Urban parks provide ecosystem services by retaining metals and nutrients in soils. Environmental Pollution, 231, 451–461.
Speak, A. F., Mizgajski, A., & Borysiak, J. (2015). Allotment gardens and parks: Provision of ecosystem services with an emphasis on biodiversity. Urban Forestry and Urban Greening, 14(4), 772–781.
Talal, M. L., & Santelmann, M. V. (2020). Vegetation management for urban park visitors: A mixed methods approach in Portland, Oregon. Ecological Applications, 30(4), e02079.
Westhoff, V., & Van Der Maarel, E. (1978). The Braun-Blanquet approach. In: Whittaker, R. H. (Ed.). Classification of plant communities. Springer Netherlands. Pp. 287–399.
Williams, N. S. G., Hahs, A. K., & Vesk, P. A. (2015). Urbanisation, plant traits and the composition of urban floras. Perspectives in Plant Ecology, Evolution and Systematics, 17(1), 78–86.
Xing, Y., & Brimblecombe, P. (2019). Role of vegetation in deposition and dispersion of air pollution in urban parks. Atmospheric Environment, 201, 73–83.
Yorkina, N., Goncharenko, I., Lisovets, O., & Zhukov, O. (2022). Assessment of naturalness: The response of social behavior types of plants to anthropogenic impact. Ekológia (Bratislava), 41(2), 135–146.
Yorkina, N., Maslikova, K., Kunah, O., & Zhukov, O. (2018). Analysis of the spatial organization of *Vallonia pulchella* (Muller, 1774) ecological niche in technosols (Nikopol Manganese Ore Basin, Ukraine). Ecologica Montenegrina, 17(1), 29–45.
Zhang, Y., Li, P., Liu, X., & Xiao, L. (2022). Changes in soil aggregate fractions, stability, and associated organic carbon and nitrogen in different land use types in the Loess Plateau, China. Sustainability, 14(7), 3963.
Zhu, W., Sun, J., Yang, C., Liu, M., Xu, X., & Ji, C. (2021). How to measure the urban park cooling island? A perspective of absolute and relative indicators using remote sensing and buffer analysis. Remote Sensing, 13(16), 3154.
Zhukov, A., & Gadorozhnaya, G. (2016). Spatial heterogeneity of mechanical impedance of a typical chernozem: The ecological approach. Ekológia (Bratislava), 35(3), 263–278.
Zhukov, O. V., Kunah, O. M., Dubinina, Y. Y., Fedushko, M. P., Kotsun, V. I., Zhukova, Y. O., & Potapenko, O. V. (2019). Tree canopy affects soil macrofauna spatial patterns on broad- and meso-scale levels in an Eastern European poplar-willow forest in the floodplain of the River Dnipro. Folia Oecologica, 46(2), 101–114.
Zhukov, O., Kunakh, O., Yorkina, N., & Tutova, A. (2023). Response of soil macrofauna to urban park reconstruction. Soil Ecology Letters, 5(2), 220156.